domain (GAL4 DNA-binding domain), Sall1 protein is capable of repressing transcription on the synthetic reporter containing tandem GAL4-binding sites upstream of a promoter. The native DNA-binding site and direct target genes regulated by Sall1 proteins have remained to be determined.

In *Drosophila* wing development, *sal* is activated downstream of *dpp* (bone morphogenetic protein 4 ortholog) and in tracheal development is activated downstream of *wingless* (Wnt ortholog) [5,21–23]. We did research to determine if mammalian Sall1 is involved in signaling pathways related to development. We report here that Sall1 synergistically enhanced reporter activities of the canonical Wnt signal, by localizing to heterochromatin. Our evidence indicates that this mechanism may be related to the cause of TBS.

Materials and methods

Plasmids. The complete coding *Sall1* cDNA was fused to the HA-tag by replacing the PCR fragment amplified using the primer containing HA-tagged sequence and the *SalI* restriction enzyme site (f, GTCGACCCATGTACCCATACGACGTCCCAGACTACGCTTCGCGGAGGAAGCAAGCG; r, GAGCAGAAGGTCTGATAATTC). The *SalI–NotI* digested HA-tagged *Sall1* cDNA fragment was cloned into the *XhoI–NotI* sites of pCAGEN, a mammalian expression vector driven by the CAG promoter [24,25].

Sall1 truncated forms were generated as follows; zinc finger region 1 (Zn 1) encoding 1–288 amino acids (*SalI-SacI* fragment) was inserted into pCAGEN vector, zinc finger region 2 (Zn 2) encoding 289–598 amino acids (*SacI–ApaI* fragment), zinc finger region 3 (Zn 3) encoding 599–857 amino acids (*ApaI–XhoI* fragment), zinc finger region 4 (Zn 4) encoding 858–1105 amino acids (*XhoI–SpeI* fragment), and zinc finger region 5 (Zn 5) encoding 1106–1324 amino acids (*SpeI–NotI* fragment) were inserted into appropriate restriction sites in pCMV-HA vector (Clontech). The N-terminal half form of HA-tagged Sall1 encoding 1–598 amino acids (Zn1-2) was inserted into the pCAGEN vector, and the C-terminal half form encoding 599–1324 amino acids (Zn 3–5) inserted into the pCMV-HA vector.

The Sall1-GFP fusion was generated by inserting the d2EGFP fragment from pd2EGFP-1 vector (Clontech) at the 3′ terminal region of Sall1 in pBluescript II KS (−) vector in-frame. *SalI–NotI* fragment of the Sall1-d2EGFP fusion was excised and inserted into the pCAGEN vector. To generate GFP-fused Sall1 truncated forms, the pCMV-HA-NLS-d2GFP vector was constructed. The PCR fragment coding a single nuclear localization signal from SV40 was inserted into the pCMV-HA vector (pCMV-HA-NLS vector) and then the fragment coding d2EGFP following intact multiple cloning sites excised from pd2EGFP-1 vector was inserted and the pCMV-HA-NLS-d2EGFP vector was generated. Sall1 truncated forms fused to d2EGFP were generated as follows; zinc finger region 1 encoding 1–288 amino acids (*SalI–SacI* fragment), zinc finger region 1–2 encoding 1–598 amino acids (*SacI–ApaI* fragment), and zinc finger region 3–5 encoding 599–1324 amino acids (*SpeI–NotI* fragment) were inserted into appropriate restriction sites in pCMV-HA-NLS-d2EGFP vector (Clontech) in-frame. The cDNA fragment of zinc finger region 1′ (Zn 1′) encoding 1–435 amino acids was generated by the combination of the *SalI–SacI* fragment encoding 1–288 amino acids and the fragment encoding 299–435 amino acids that was amplified using primers containing *SmaI* restriction enzyme site in the reverse one (f, ATTAGC ACAGAGCCTTGCTAGC; r, CCCGGGGGACATTTGG TGGCTTGCTTTTTC). The combined cDNA fragment was inserted into the pCMV-HA-NLS-d2EGFP vector in-frame. The cDNA encoding zinc finger region 1′ (1–435 amino acids) without NLS was generated by combination of the *SalI–SacI* fragment encoding 1–288 amino acids and the fragment encoding 299–435 amino acids fused to d2EGFP, which was excised from the pCMV-HA-NLS-Zn 1′-d2EGFP vector, as described above, and inserted into appropriate sites in the pCAGEN vector. To generate the Zn 1′-DsRed2 fusion, the *AgeI–XhoI* DsRed2 fragment without NLS was excised from pDsRed2-Nuc vector (Clontech), and inserted into the pCAGEN vector with the *SalI–AgeI* Zn 1′ fragment excised from the pCMV-HA-NLS-Zn 1′-d2EGFP vector.

The fragment coding the complete β-catenin cDNA was excised from pBJ-myc-β-catenin by *Bam*HI [26] and inserted into appropriate sites in the pCMV-myc vector (Clontech).

Protein interaction assay. BOSC23 cells were transiently transfected with 4 μg pCAGEN-HA-Sall1 or each pCMV-HA-Sall1 truncated form and 3 μg pCMV-myc-β-catenin. After 48 h, cells were washed with phosphate-buffered saline, lysed for 10 min on ice with 600 μl buffer A (10 mM Hepes–KOH, pH 7.8, 10 mM KCl, 1.5 mM $MgCl_2$, 0.05% NP-40, 0.5 mM DTT, and 10% v/v protease inhibitor cocktail for mammalian cell extract (SIGMA)), and spun at 2300*g* for 1 min. The supernatant was discarded and then the pellet was suspended in 300 μl buffer C (20 mM Hepes–KOH, pH 7.8, 500 mM NaCl, 1.5 mM $MgCl_2$, 0.5 mM DTT, and 10% v/v protease inhibitor cocktail for mammalian cell extract), rotated at 4 °C for 30 min and then spun at 20,000*g* for 30 min. The supernatant was diluted with an equal volume of buffer C containing 50% glycerol.

For the immunoprecipitation assay, the extract was diluted with an equal volume of buffer D (20 mM Hepes–KOH, pH 7.8, 1.5 mM $MgCl_2$, 0.5 mM DTT, and 10% v/v protease inhibitor cocktail for mammalian cell extract), twice the volume of the dilution buffer (25 mM Hepes–KOH, pH7.8, 2.5 mM EDTA, 0.1% NP-40, and 10% v/v protease inhibitor cocktail for mammalian cell extract) in a 1.5 ml micro tube and then incubated on ice for 10 min. After removal of particulate cell debris by centrifugation at 20,000*g* for 5 min, the supernatant was incubated overnight with 2 μg of anti-HA high affinity (Roche) at 4 °C. HA-tagged protein and its interacting proteins were isolated by precipitation with protein G–Sepharose beads (Amersham–Pharmacia) for 3 h at 4 °C. The beads were washed three times with wash buffer (20 mM Hepes–KOH, pH 7.8, 375 mM NaCl, 1 mM $ZnCl_2$, 1 mM EDTA, 0.5 mM DTT, 1% NP-40, 10% glycerol, and 1 mM PMSF) and eluted by boiling in Laemmli sample buffer. HA-tagged protein and its interacting proteins were separated by SDS–polyacrylamide gel electrophoresis on 8% gels, transferred to Immobilon Transfer Membranes (Millipore), blocked in 3% nonfat dried milk, and incubated with anti-HA antibody (Roche) or anti-myc antibody (SC-40, Santa Cruz Biotechnology). Antibody reactivity was detected using horseradish peroxidase-labeled secondary antibodies anti-mouse (KPL) and horseradish peroxidase-labeled secondary antibodies anti-rat (KPL) and ECL detection reagents (Amersham–Pharmacia).

Monoclonal antibody for human SALL1. To generate a monoclonal antibody for human SALL1, we cloned the cDNA fragment of human SALL1 encoding 258–499 amino acids amplified using primers containing *KpnI* restriction site at the 5′ end (f, GGTACCCGCTTCT CAGAATGCAGACTTG; r, GGTACCTTGTGTTTGAAGAATGC CTC). The PCR fragment was cloned into the *KpnI* sites of pBACsurf-1, which is a baculovirus transfer vector designed for expression of target proteins on the virion surface. Recombinant virus was produced, purified, and then immunized [27]. Monoclonal antibody for human SALL1 was obtained after screening by immunoblotting using the extract from HEK293 cells. These selected clones were cross-reactive for both human SALL1 and mouse Sall1 proteins.

Cell culture, transfection, and RNAi. NIH-3T3 cells and HEK293 cells were maintained in Dulbecco's modified Eagle's medium (SIGMA) containing 10% fetal bovine serum. For reporter assay, cells were plated in a 6-well plate at a density of 1×10^5 cells per well. For transfection of plasmids, FuGENE6 (Roche Molecular Biochemicals) was used according to the manufacturer's direction. For transfection

of double-stranded (ds) RNA oligos, LIPOFECTAMINE 2000 (Invitrogen) was used according to the manufacturer's direction. Five ds RNAi oligos for SALL1 were designed and synthesized by DHARMACON. Sequences of these oligos are as follows:

No. 6 (5′-AAGGUCUUUGGGAGUGACAGU-3′),
No. 7 (5′-AAGAGAAAUACCCUCAUAUCC-3′),
No. 15 (5′-AAUGAUUCAUCCUCAGUGGGU-3′),
No. 18 (5′-AAGGGUAAUUUGAAGCAGCAC-3′),
No. 21 (5′-AAGUUCCCAGAAAUGUUCCAG-3′).

The probe used for Northern blots was the *Kpn*I fragment of human SALL1 cDNA, excised from the pBACsurf-human SALL1 vector described above. For Western blotting, we used a monoclonal antibody for human SALL1 as described and a monoclonal antibody for GAPDH (Ambion).

Reporter assay. An internal control reporter pRLTKmini, which has the minimal thymidine kinase promoter, was constructed by removing the *Bgl*II–*Eco*RI fragment from the promoter region of pRLTK (Promega). TOPflash (Upstate Biotechnology) is a luciferase reporter containing three copies T cell factor (TCF) binding sites upstream of the thymidine kinase minimal promoter and FOPflash (Upstate Biotechnology) is the negative control for TOPflash containing mutant TCF binding sites. In the reporter assay using Wnt supernatant, 0.5 μg TOPflash or FOPflash reporter plasmid, 0.05 μg pRLTKmini control reporter plasmid were transiently introduced with 1.0 μg Sall1 or Sall1 truncated mutant expression plasmids in NIH3T3 cells. In the reporter assay using HEK293 cells, the same amounts of reporters were introduced with 0.1 μg pCAGEN-HA-Sall1. In the reporter assay using the N-terminal truncated Sall1 (Zn 1′) plasmid, 0.1–1.0 μg of this plasmid was transiently introduced with 0.1 μg pCAGEN-HA-Sall1 in HEK293 cells. After 24 h, the transfected cells were stimulated by threefold-diluted Wnt supernatants, produced from Wnt3a overexpressing L cells (ATCC) [28]. After 48 h, the transfected cells were lysed with 150 μl lysis buffer (50 mM Tris–HCl, pH 7.4, 150 mM NaCl, 1 mM EDTA, and 0.1% NP-40), frozen and thawed three times, and then spun at 20,000*g* for 10 min. The supernatant was then assayed using Dual-Luciferase Reporter Assay System (Promega). Luminescent reporter activity was measured using LUMAT LB 9507 luminometer (EG&G BERTHOLD). In the reporter assay using the β-catenin expression vector, 0.3 μg pCMV-myc-β-catenin with 0.1–1.0 μg pCAGEN-HA-Sall1 was transiently introduced into NIH3T3 cells. In HEK293 cells, 0.01 μg pCMV-myc-β-catenin with 0.01–0.1 μg pCAGEN-HA-Sall1 was used. Forty-eight hours after transfections, cells were used in the same way as described above. In the reporter assay combined with RNA interference, the final concentration 20 μM of each si RNA oligo was transfected in Opti-MEM (Invitrogen) as the serum free condition using LIPOFECTAMINE 2000 (Invitrogen). After 6 h, the serum free medium was replaced with Dulbecco's modified Eagle's medium (SIGMA) containing 10% fetal bovine serum, then reporter plasmids were transfected in the same way as described above. In all reporter assays, EGFP expression plasmid, pCMV-EGFP, was used to normalize the DNA content of the transfection. All transfections were normalized to *Renilla* luciferase activity and were replicated. All reporter assays were repeated at least three times and representative data are shown.

Analysis of protein localization by confocal microscopy and immunocytochemistry. Total 1.0 μg of Sall1-GFP fusion plasmid or Sall1 mutant GFP fusion plasmids or β-catenin plasmid was transiently introduced into NIH3T3 cells plated in Lab-Tek II Chamber Slide w/ Cover RS Glass Slide (Nalge Nunc International). Twenty-four hours after transfection, cells were fixed in phosphate-buffered saline (PBS) containing 2% paraformaldehyde, 0.1% Triton X-100, and 2 μg/ml of 4,6-diamidino-2-phenylindole (DAPI) at 4 °C for 20 min, washed for 5 min in PBS three times at room temperature, and then blocked with 10% goat serum at room temperature for 30 min. Cells were then incubated for 1 h at room temperature with an anti-myc antibody diluted in PBS containing 1% goat serum (1:1000), and detected using a rhodamine-conjugated secondary antibody anti-mouse (CHEMICON). The localization of proteins was detected using confocal microscopy Radiance 2100 (Bio-Rad).

Results

Sall1 has the potential to activate the canonical Wnt signaling

As the expression of *spalt* is regulated by several signaling pathways (*dpp*/BMP, *wingless*/Wnt, etc.) in *Drosophila* development, luciferase assays were done using several reporters to examine the potential involvement of mammalian Sall1. In following experiments, we selected and used two cell lines; NIH3T3 cells and HEK293 cells. Endogenous Sall1 was detected in HEK293 cells, in RNA and protein levels, but not in NIH3T3 cells (data not shown). Among reporters tested (BMP, TGF-β, retinoic acid, LIF, and Wnt) [25,29–32], the Wnt responsive reporter consistently showed a synergistic response to Sall1 (Figs. 1A and B) in both cell lines. Sall1 expression vector was introduced with the Wnt responsive reporter (TOPflash) that contains multiple TCF binding sites or the control reporter (FOPflash), and these cells were stimulated by the supernatant from L cells stably expressing Wnt-3A. Sall1 alone only weakly activated the TOPflash reporter in both cell lines. In the presence of Wnt stimulation, however, Sall1 synergistically activated the TOPflash reporter in both cell lines, but not so the control FOPflash reporter. Therefore, Sall1 synergistically activates the canonical Wnt signal. In these settings, activation status of β-catenin was not altered as determined by Western blotting, ruling out the possibility of a secondary production of Wnt ligands by Sall1 or Wnt stimulation upstream of β-catenin (data not shown).

When the canonical Wnt pathway is activated, β-catenin avoids the ubiquitin–proteosome pathway following the phosphorylation by GSK3-β and accumulates in the cytoplasm to move into the nucleus and function as the transcriptional coactivator of the TCF/LEF transcription factor [33]. In NIH3T3 cells, expression of β-catenin alone activated gene expression on the TOPflash reporter only slightly, but co-expression of Sall1 and β-catenin synergistically increased its reporter activity in dependent manner regarding the amount of Sall1 (Fig. 1C). In HEK293 cells, Sall1 also enhanced the luciferase reporter by β-catenin (Fig. 1D). Sall1 by itself could not bind to TCF binding sites in the TOPflash reporter, as determined by an electromobility shift assay using nuclear extracts from Sall1-introduced HEK293 cells (data not shown). Therefore, Sall1 may possibly function as a coactivator for β-catenin in the canonical Wnt signaling.

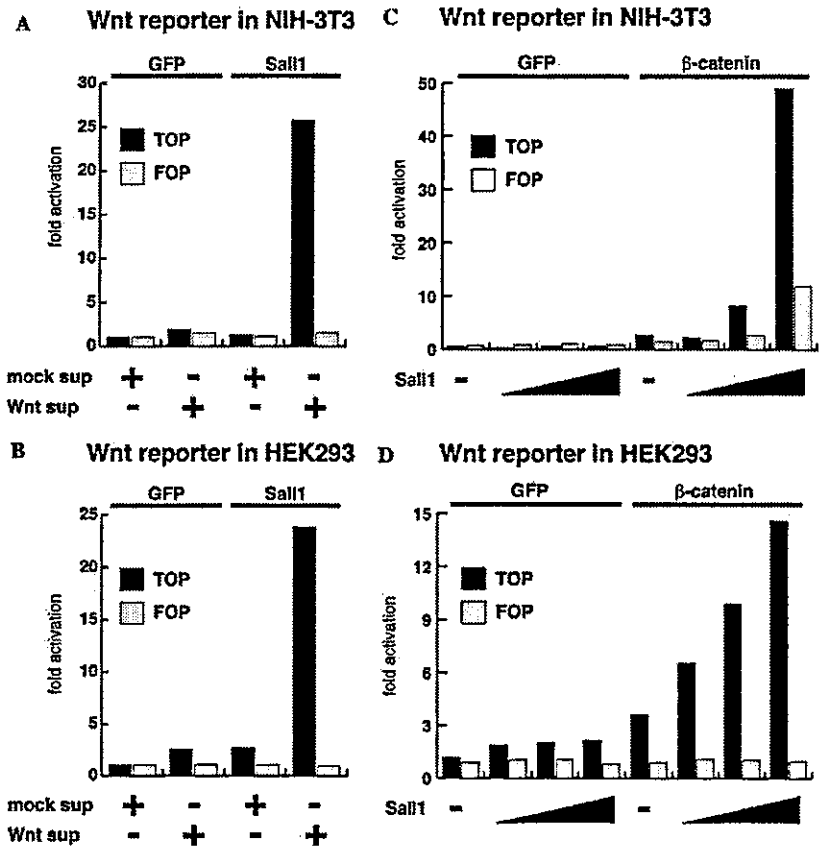

Fig. 1. Sall1 synergistically enhanced canonical Wnt signaling pathway. (A,B) The reporter assay responsive to Wnt signaling. TOPflash as the reporter plasmid responsive to Wnt signaling, FOPflash as negative control were introduced into NIH-3T3 cells (A), HEK293 cells (B). These cells were stimulated by the Wnt supernatant (Wnt sup) from L cell stably expressing Wnt-3A or the mock supernatant (mock sup) from normal L cells. (C,D) TOPflash reporter assay by expression of β-catenin, with or without Sall1. pCMV-myc-β-catenin (0.3 μg) (the β-catenin expression vector) and 0.1–1.0 μg of pCAGEN-HASall1 were introduced in NIH-3T3 cells (C). pCMV-myc-β-catenin (0.01 μg) (the β-catenin expression vector) and 0.01–0.1 μg of pCAGEN-HASall1 were introduced in HEK293 cells (D). In all reporter assays, pCMV-EGFP (the control vector) was used to normalize the DNA content of the transfection, and pRLTKmini was used as the internal control reporter plasmid.

Endogenous Sall1 participates in Wnt signaling in HEK293 cells

To determine if Sall1 endogenously participates in canonical Wnt signaling, we depleted the endogenous human SALL1 protein in HEK293 cells via double-strand RNA (siRNA)-mediated interference and did reporter assays. We designed five kinds of ds RNAi oligos for human SALL1 (Nos. 6, 7, 15, 18, and 21), and assessed their potential to deplete endogenous SALL1 mRNA, using Northern blot analysis (Fig. 2A). Oligo No. 18 most effectively, and Nos. 6 and 7 weakly, reduced endogenous SALL1 mRNA in HEK293 cells, but No. 21 had no effect (Fig. 2A). Therefore, we selected No. 21 as a negative control in following experiments, as it did not reduce the amount of either SALL1 or GAPDH (Figs. 2B and C). When used in reporter assays, oligo No. 18 most effectively, oligo No. 6 less effectively, down-regulated the activity on the TOPflash reporter, in proportion to their efficiency to reduce endogenous SALL1 mRNA, while a negative control, No. 21, did not do so (Fig. 2D). Therefore, endogenous SALL1 also participates in canonical Wnt signaling, at least in HEK293 cells.

Sall1 interacts with β-catenin

We next did immunoprecipitation studies to examine the interaction between Sall1 and β-catenin. Nuclear extracts were prepared from BOSC23 cells, transiently introduced with both HA-tagged Sall1 and myc-tagged β-catenin expression vectors. In these extracts, Sall1 effectively interacted with β-catenin (Fig. 3B). To further determine the domains of Sall1 required for interactions with β-catenin, we also did immunoprecipitation studies using deletion mutants of Sall1 with β-catenin. Sall1 has a total of 10 zinc fingers including multiple double-zinc finger motifs and we constructed five truncated mutants

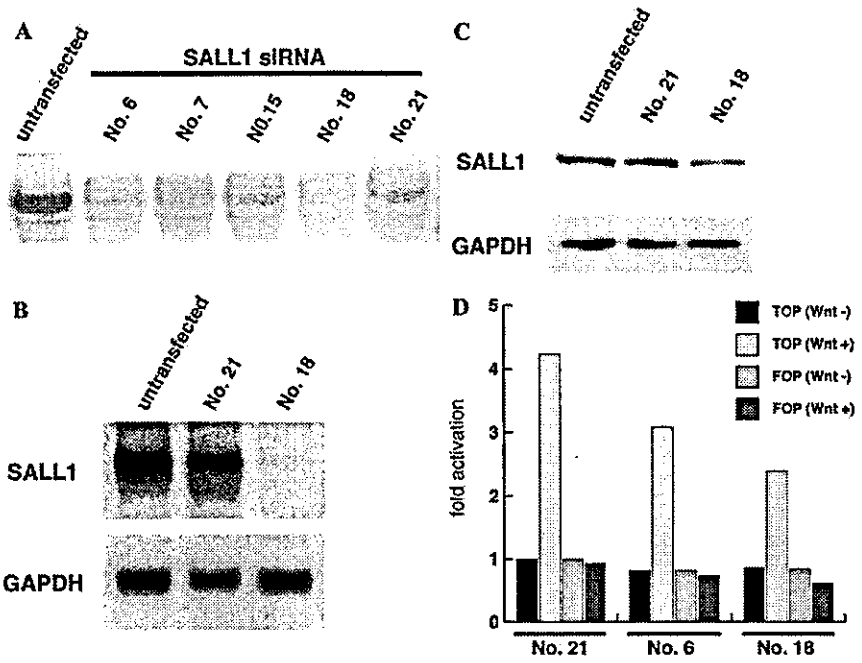

Fig. 2. RNA interference for endogenous Sall1 specifically down-regulates the TOPflash activity in HEK293 cells. (A,B) Northern analysis for assessing the efficiency of five designed siRNA oligos for human SALL1 to reduce the amount of endogenous SALL1 mRNA. (C) Western analysis for assessing the efficiency of SALL1 siRNA oligos to reduce the amount of endogenous SALL1 protein. (D) The reporter assay using SALL1 siRNA oligos in HEK293 cells. siRNA oligo, No. 18 most efficiently, and No. 6 less efficiently, down-regulated the reporter activity on TOPflash reporter in proportion to its efficiency to reduce endogenous SALL1 mRNA, while No. 21 had no effect.

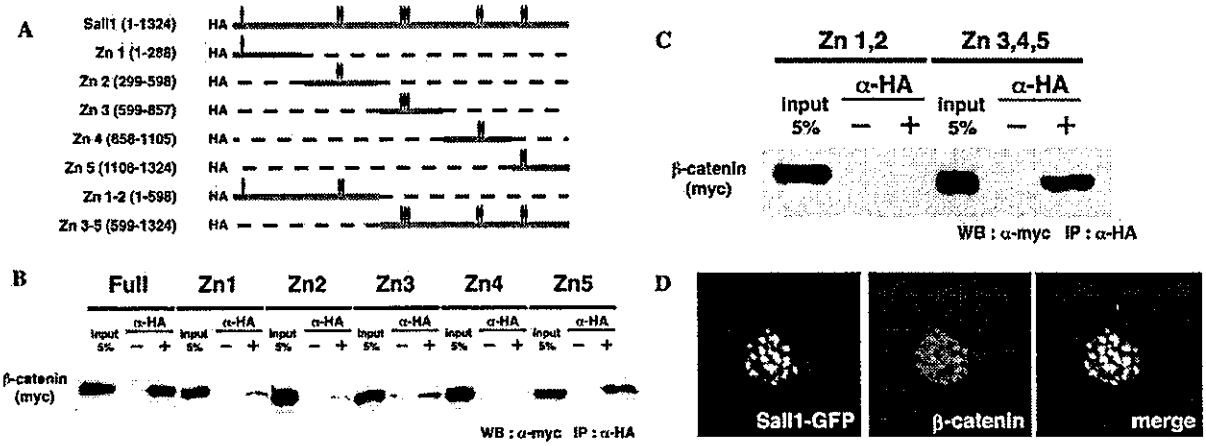

Fig. 3. Localization of Sall1, which has the potential to associate with β-catenin, does not overlap with those of β-catenin in the nucleus. (A) Diagram of HA-tagged full-length Sall1 and its deletion mutants used in protein interaction assays. Positions of the zinc fingers are depicted as ovals. The numbers in parentheses indicate the number of coding amino acids. (B,C) Protein interaction assay by immunoprecipitation using nuclear extracts from BOSC23 cells, transiently introduced with myc-β-catenin and HA-Sall1 or its mutants. Immunoprecipitation was done using an anti-HA antibody and detected using an anti-myc antibody. (D) The localization of Sall1 in the nucleus did not overlap with that of β-catenin. NIH3T3 cells on glass coverslips were transfected with full-length Sall1-GFP and myc-tagged β-catenin, stained with anti-myc. Cells were viewed using confocal microscopy.

encoding clusters of each zinc finger motif (Zn 1, 2, 3, 4, and 5) (Fig. 3A). The immunoprecipitation was done using lysates from BOSC23 cells introduced with these truncated mutants and β-catenin. The truncated form, encoding the most C-terminal double-zinc finger (Zn 5), had the highest affinity with β-catenin, and the form encoding the triple Zn finger (Zn 3) had a lesser affinity for β-catenin (Fig. 3B). To confirm these results, we

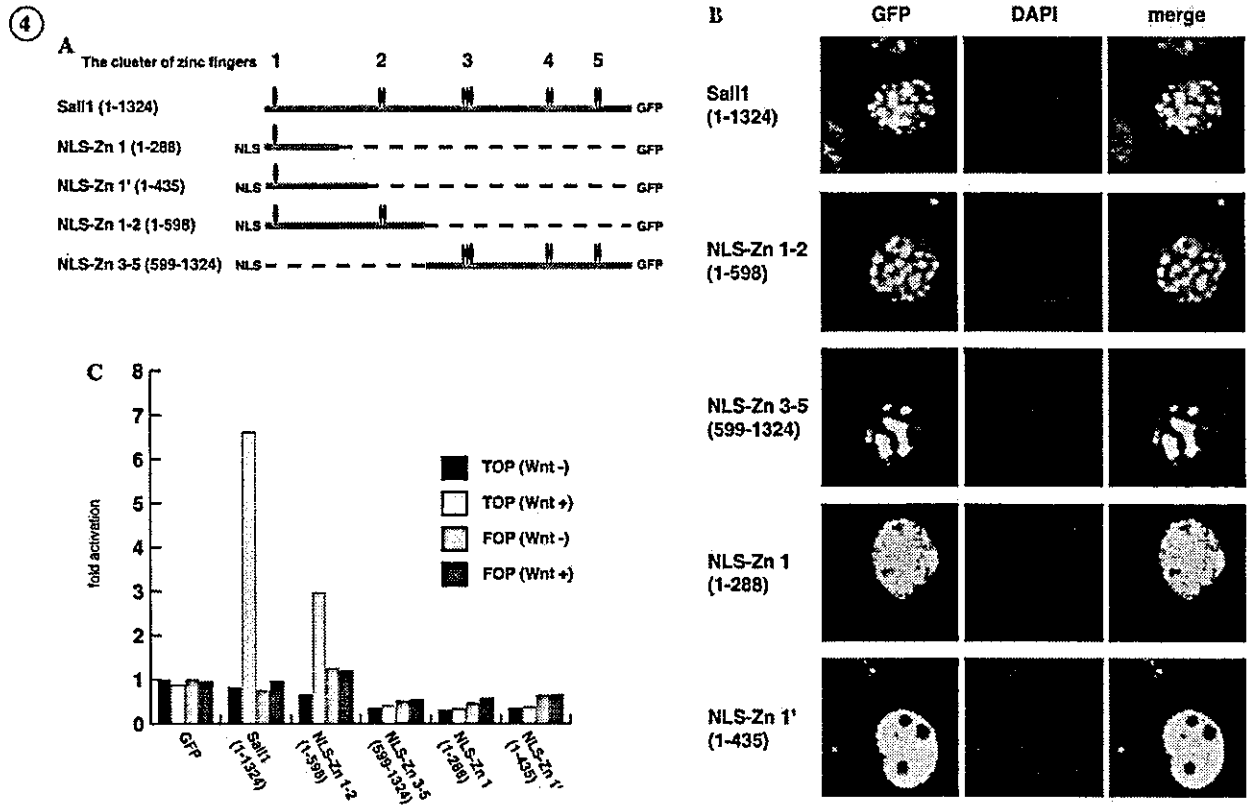
4
A
The cluster of zinc fingers 1 2 3 4 5
Sall1 (1-1324)
NLS-Zn 1 (1-288)
NLS-Zn 1' (1-435)
NLS-Zn 1-2 (1-598)
NLS-Zn 3-5 (599-1324)
NLS
GFP
B
GFP
DAPI
merge
Sall1 (1-1324)
NLS-Zn 1-2 (1-598)
NLS-Zn 3-5 (599-1324)
NLS-Zn 1 (1-288)
NLS-Zn 1' (1-435)
C
fold activation
TOP (Wnt-)
TOP (Wnt+)
FOP (Wnt-)
FOP (Wnt+)
GFP
Sall1 (1-1324)
NLS-Zn 1-2 (1-598)
NLS-Zn 3-5 (599-1324)
NLS-Zn 1 (1-288)
NLS-Zn 1' (1-435)

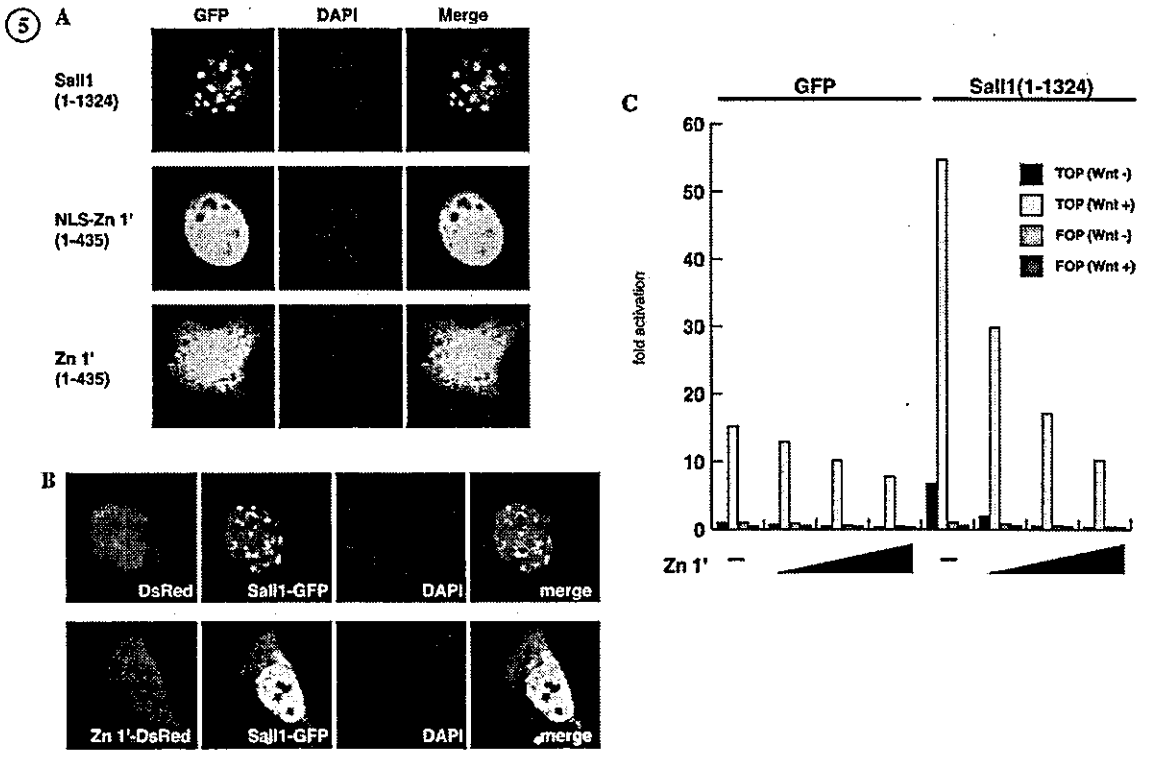
5
A
GFP
DAPI
Merge
Sall1 (1-1324)
NLS-Zn 1' (1-435)
Zn 1' (1-435)
B
DsRed
Sall1-GFP
DAPI
merge
Zn 1'-DsRed
Sall1-GFP
DAPI
merge
C
GFP
Sall1(1-1324)
fold activation
TOP (Wnt-)
TOP (Wnt+)
FOP (Wnt-)
FOP (Wnt+)
Zn 1'

divided Sall1 into halves and constructed two other mutant forms; Zn 1–2, the N-terminal half of Sall1, encoded first and second Zn finger regions, and Zn 3–5, the C-terminal half, encoded third, fourth, and fifth Zn finger regions (Fig. 3A). β-Catenin strongly interacted with the C-terminal half domain encoding Zn 3–5, but not with the N-terminal half domain encoding Zn 1–2 (Fig. 3C).

We next assessed whether the localization of Sall1 in the nucleus correlated with those of β-catenin in NIH3T3 cells, because NIH3T3 cells were useful to distinguish between euchromatic and heterochromatic regions than in HEK293 cells by confocal microscopy. Sall1 was localized to punctate nuclear foci (pericentromeric heterochromatin) as reported [19,20]. β-Catenin in the nucleus was also localized to the punctate nuclear foci, but its localization pattern only partially overlapped with Sall1 (Fig. 3D). This suggests that not all Sall1 in nucleus associates with β-catenin. We also assessed whether, upon Wnt stimulation, the localization pattern of Sall1 changes to overlap with that of β-catenin. Sall1 localization, however, did not change with or without Wnt stimulation (data not shown). Thus, Sall1 is not a simple coactivator for β-catenin on the TOPflash reporter.

The transcriptional activity of Sall1 correlates with its localization in the nucleus

Recently, Sall1 was reported to localize to punctate nuclear foci (pericentromeric heterochromatin) and its nuclear localization to correlate with its transcriptional repression [19,20]. We categorized 10 zinc fingers of Sall1 to five clusters of zinc fingers (Zn 1, 2, 3, 4, and 5) (Fig. 4A). To assess whether the localization of Sall1 in the nucleus also correlates with its transcriptional activation in Wnt signaling, we constructed Sall1-GFP or Sall1 mutants-GFP (Fig. 4A) and examined localization of these GFP-fusion proteins in NIH-3T3 cells using confocal microscopy (Fig. 4B). To focus localization of those mutants only in nucleus, the nuclear localization signal from SV40 was fused to the N-terminal of each GFP-fusion mutant. The full-length Sall1-GFP was localized as a small speckled pattern in the nucleus and co-localized with 4,6-diamidino-2-phenylindole (DAPI) and heterochromatin protein 1 (HP1), as reported [19,20] (Fig. 4B and data not shown). The N-terminal half of Sall1, Zn 1–2, was also localized in a similar fashion to the full-length Sall1, but localization of the C-terminal half, Zn 3–5, looked different; larger speckles or aggregates than those of the full-length and N-terminal half of Sall1-GFP (Fig. 4B). It was reported that the most N-terminal zinc finger domain that binds to HDAC complex is essential and sufficient for its repressor activity [19]. Therefore, we constructed Zn 1′ encoding 1–435 amino acids, which was reported to be the minimal truncated form as a transcriptional repressor (Fig. 4A). Unexpectedly, Zn 1′, which was reported to localize to heterochromatin in COS-1 cells, showed a uniform localization in the nucleus (Fig. 4B). The most N-terminal single zinc finger region, Zn 1, also showed uniform localization in the nucleus (Fig. 4B). Therefore, its localization to heterochromatin requires both the N-terminal single zinc finger (Zn 1) and the following double zinc fingers (Zn 2).

We next did luciferase reporter assays using full-length Sall1 protein and these Sall1 truncated forms. NIH-3T3 cells, introduced with these truncated Sall1 expression plasmids and TOPflash reporter, were stimulated by Wnt supernatants (Fig. 4C). Interestingly, Zn 3–5 (C-terminal half), that has the potential to bind β-catenin, had no activity in the luciferase assay. In contrast, Zn 1–2 (N-terminal half), that has the capacity to localize to heterochromatin, activated the TOPflash reporter, regardless of no interaction with β-catenin (Figs. 3B and C). This indicates Sall1 localization to heterochromatin, but not its association with β-catenin, correlates with its transcriptional activation in Wnt signaling. As Zn 1 and Zn 1′, which have only the first zinc finger, did not show synergistic enhancement of the reporter activity nor localization to heterochromatin, both zinc finger regions 1 and 2 are required for localization to heterochromatin and its synergistic transcriptional enhancement in Wnt signaling.

Fig. 4. The N-terminal half region of Sall1 has the potential to be localized to heterochromatin and to enhance synergistically Wnt reporter activity. (A) Diagram of GFP fused full-length Sall1 and its deletion mutants used in the confocal microscopy. Mutants are fused to NLS in N-terminus and to EGFP in C-terminus. (B) NIH3T3 cells grown on glass coverslips were transfected with corresponding deletion mutants of Sall1-GFP (green) or Sall1-truncated mutants-GFP, counterstained with DAPI (blue) to identify heterochromatin in nucleus, and viewed using confocal microscopy. (C) The reporter assay responsive to Wnt signaling using Sall1-GFP or Sall1 mutants-GFP plasmids. NIH3T3 cells were transfected with 1.0 μg of each Sall1-GFP or Sall1 mutants-GFP, and after 24 h, stimulated with Wnt sup or the mock sup.

Fig. 5. Zn 1′, which is produced by mutations often observed in human TBS, disrupts the localization of native Sall1 protein and its transcriptional activity in Wnt signaling in a dominant-negative fashion. (A) NIH3T3 cells were transfected with corresponding deletion mutants of Sall1-GFP (green), NLS-Zn 1′-GFP, or Zn 1′-GFP without NLS, and stained with DAPI (blue), and viewed using confocal microscope. (B) Full-length Sall1-GFP was introduced into NIH3T3 cells, together with DsRed (upper panels) or Zn 1′-DsRed (lower panels). DAPI staining (blue) shows heterochromatin. (C) The reporter assay responsive to Wnt signaling using the N-terminal truncated mutant Zn 1′. HEK293 cells were transfected with 0.1–1.0 μg Zn 1′ plasmid with or without 0.1 μg HA-Sall1 plasmid in addition to reporter plasmids, and after 24 h, stimulated by the Wnt sup or the mock sup.

Zn 1′, which is produced by mutations often observed in human TBS, disrupts the localization of native Sall1 protein and its transcriptional activity in Wnt signaling in a dominant-negative fashion

It was recently reported that mice carrying a mutation which caused the production of the truncated Sall1 protein, Zn 1′, recapitulated the abnormalities found in human TBS [34,35]. We confirmed that Zn 1′-GFP protein without NLS was localized uniformly in the cytoplasm and in the nucleus, as reported (Fig. 5A). As Zn 1′ was also reported to associate with all Sall family members, probably through the conserved N-terminal glutamine-rich domain [34,36], we hypothesized that Zn 1′ without NLS may affect the localization of native Sall1 protein and its synergistic enhancement of Wnt signaling. We constructed Zn 1′ protein fused to DsRed, introduced it with full-length Sall1-GFP fusion in NIH-3T3 cells, and examined the localization of these proteins using confocal microscopy. When co-expressed with the control DsRed protein, full-length Sall1-GFP remained to be localized to heterochromatin (Fig. 5B). Zn 1′ fused to DsRed, however, affected the localization of Sall1-GFP; Sall1-GFP was localized in both the cytoplasm and the nucleus. Sall1-GFP in the nucleus was no longer localized to heterochromatin, being uniformly localized together with Zn 1′-DsRed (Fig. 5B). This indicates that Zn 1′ functions as a dominant-negative form for native Sall1 proteins, by inhibiting the native Sall1 from localizing to heterochromatin. To assess whether Zn 1′ also functions as the dominant-negative form in Wnt signaling, we next did luciferase reporter assays of HEK293 cells using the Zn 1′ truncated forms without NLS. As HEK293 cells express endogenous Sall1, Zn 1′ introduction down-regulated the activity of endogenous Sall1 on the TOPflash reporter in a dose-dependent manner (Fig. 5C). When introduced with exogenous native Sall1, Zn 1′ also efficiently inhibited synergistic activation of the Wnt responsive reporter by native Sall1 (Fig. 5C). This indicates that the N-terminal truncated Sall1, Zn 1′, which is caused by high-frequent mutations in TBS, also functions as a dominant-negative form in canonical Wnt signaling. We propose that this newly defined mechanism of Wnt signaling activation by heterochromatin localization of Sall1 may explain one of the causative mechanisms of TBS.

Discussion

Sall plays important roles in a variety of organs, but its molecular mechanisms have remained largely unknown.

Here we show that Sall1 functions as a transcriptional activator specifically in the canonical Wnt signaling pathway. The luciferase activity on the TOPflash reporter stimulated by Wnt-3a was synergistically activated by the introduction of Sall1 (Fig. 1). We also tested other unrelated zinc finger proteins on the TOPflash reporter, and found that the effect on Wnt canonical pathway was specific to Sall1 (data not shown). The synergistic activity on TOPflash reporter by Sall1 was also observed by transfection of β-catenin and Sall1. The introduction of ds RNAi oligo for human SALL1 to HEK293 cells not only reduced the amount of endogenous SALL1 protein, but also led to down-regulation of the TOPflash reporter activity (Fig. 2). Activation of Wnt signaling by Sall1 did not correlate with its localization with β-catenin, but rather with its localization of heterochromatin (Figs. 3 and 4). Further, the N-terminal truncated form of Sall1 (Zn 1′), which was reported to lead human TBS abnormalities in mice [34], disturbed localization of the native Sall1 and also down-regulated the synergistic activity on TOPflash reporter by native Sall1 (Fig. 5).

In two previous reports, Sall1 was seen to function as a transcriptional repressor on the artificial promoter containing tandem GAL4 binding sites, when linked to the heterologous GAL4 DNA-binding domain, and also that Sall1 associated with HDAC and several components of the chromatin remodeling complex (MTA1, MTA2, and RbAp46/48) [20,34]. Therefore, Sall1 could repress gene expression by recruiting the HDAC complex. It was not, however, reported that native Sall1 functions as a transcriptional repressor. We found that the native form of Sall1 could function as a transcriptional activator in Wnt signaling essential for many developmental processes and that its activity correlated with its localization to heterochromatin [37]. The increase of Sall1 proteins may squelch some transcriptional repressor complex, including HDAC, or be associated with chromatin remodeling factors to alter the chromatin structure near the promoter region of Wnt target genes.

Another C2H2 type zinc finger protein Ikaros functions as both transcriptional repressor and activator, and is localized to pericentromeric heterochromatin [38–40]. Ikaros associates with DNA-dependent ATPase Mi-2 included in the NuRD chromatin remodeling complex [41]. Ikaros has six C2H2 type zinc fingers; the N-terminal zinc finger cluster consisting of four zinc fingers functions as the DNA-binding domain and C-terminal two zinc fingers as a dimerization domain [42]. When linked to a heterologous GAL4 DNA-binding domain, Ikaros functions as a transcriptional repressor on the reporter containing tandem GAL4 binding sites. On the other hand, the native form of Ikaros enhances activity of the reporter that contains tandem Ikaros binding sites upstream of the thymidine kinase promoter, and also enhances activity of the reporter containing no Ikaros binding sites but only Sp1

transcription factor binding sites. When Ikaros is not localized to heterochromatin caused by point mutations in its DNA-binding domain or dimerization domain, Ikaros does not enhance activities of these reporters. Therefore, localization of Ikaros to heterochromatin correlates with its transcriptional activation [38]. It was also reported that Sall proteins interact with all family members through its conserved glutamine-rich domain [36]. Therefore, a similar mechanism may function both for Sall1- and Ikaros-dependent activation. As the Zn 1–2 region of Sall1 was required and is sufficient for its heterochromatin localization (Fig. 4), these zinc fingers may bind to target sequences in heterochromatin, directly or indirectly. The identification of DNA sequences or molecules in heterochromatin compartments, which are required for heterochromatin localization of Sall1, would elucidate the mechanism of heterochromatin localization of Sall1 and eventually the mechanism of the activation of Wnt signaling by Sall1.

It is to be noted that Sall1-dependent activation is not general but rather it is specific to Wnt, at least among several pathways tested (BMP, TGF-β, retinoic acid, and LIF). The Wnt signal is regulated by multiple steps and large numbers of agonists and antagonists bind to β-catenin and TCF [26,43–48]. In addition, there is emerging evidence that more complicated mechanisms function in Wnt activation, including the transcriptional regulation by remodeling chromatin structure and by sumoylation [49,50]. In the former mechanism, it was reported that Brahma (Brm)/Brahma-related gene-1 (Brg-1), a component of mammalian SWI/SNF or RSC chromatin remodeling complex, binds to β-catenin, changes the chromatin structure by its ATPase activity, and then enhances Wnt-dependent transcription [49]. On the other hand, when an ARID domain protein Osa is contained in the Brm/Brg-chromatin remodeling complex, it tightens the chromatin structure and represses Wnt-dependent gene expression [50]. In the latter mechanism, the sumoylation of Lef-1 by PIASy, a member of E3 SUMO ligase, transfers Lef-1 to the nuclear body, a specific subcompartment in the nucleus, and then suppresses its transcriptional activity [51]. Tcf-4 is also sumoylated by PIASy, transferred to the PML nuclear body, and activates Wnt-dependent transcription [52]. It is to be noted that Sall1 also interacts with SUMO-1 and ubiquitin-conjugation enzyme UBE2I (human homolog of yeast UBC9), and is sumoylated [53], though its physiological relevance to Wnt signal remains to be determined. In this study, we propose another mechanism of Wnt signal activation by heterochromatin localization of Sall1. Further elucidation of this mechanism will lead to better understanding of not only the Wnt signal but also phenotypes observed in various species ranging from *Drosophila* to humans lacking SALL/spalt functions.

Acknowledgments

Akira Sato is supported by the Japan Society for the Promotion of Science. The Division of Stem Cell Regulation is supported by Amgen Limited.

References

[1] P.R. Elstob, V. Brodu, A.P. Gould, Spalt-dependent switching between two cell fates that are induced by the *Drosophila* EGF receptor, Development 128 (2001) 723–732.
[2] T.E. Rusten, R. Cantera, J. Urban, G. Technau, F.C. Kafatos, R. Barrio, Spalt modifies EGFR-mediated induction of chordontonal precursors in the embryonic PNS of *Drosophila* promoting the development of oenocytes, Development 128 (2001) 711–722.
[3] M. Boube, M. Llimargas, J. Casanova, Cross-regulatory interactions among tracheal genes support a co-operative model for the induction of tracheal fates in the *Drosophila* embryo, Mech. Dev. 91 (2000) 271–278.
[4] B. Mollereau, M. Dominguez, R. Webel, N.J. Colley, B. Keung, J.F. de Celis, C. Desplan, Two-step process for photoreceptor formation in *Drosophila*, Nature 412 (2001) 911–913.
[5] J.F. de Celis, R. Barrio, F.C. Kafatos, A gene complex acting downstream of dpp in *Drosophila* wing morphogenesis, Nature 381 (1996) 421–424.
[6] J.F. de Celis, R. Barrio, Function of the spalt/spalt-related gene complex in positioning the veins in the *Drosophila* wing, Mech. Dev. 91 (2000) 31–41.
[7] A. Buck, L. Archangelo, C. Dixkens, J. Kohlhase, Molecular cloning, chromosomal localization, and expression of the murine SALL1 ortholog Sall1, Cytogenet. Cell Genet. 89 (2000) 150–153.
[8] J. Kohlhase, M. Altmann, L. Archangelo, C. Dixkens, W. Engel, Genomic cloning, chromosomal mapping, and expression analysis of msal-2, Mamm. Genome 11 (2000) 64–68.
[9] J. Kohlhase, S. Hausmann, G. Stojmenovic, C. Dixkens, K. Bink, W. Schulz-Schaeffer, M. Altmann, W. Engel, SALL3, a new member of the human spalt-like gene family, maps to 18q23, Genomics 62 (1999) 216–222.
[10] J. Kohlhase, R. Schuh, G. Dowe, R.P. Kuhnlein, H. Jackle, B. Schroeder, W. Schulz-Schaeffer, H.A. Kretzschmar, A. Kohler, U. Muller, M. Raab-Vetter, E. Burkhardt, W. Engel, R. Stick, Isolation, characterization, and organ-specific expression of two novel human zinc finger genes related to the *Drosophila* gene spalt, Genomics 38 (1996) 291–298.
[11] T. Ott, K.H. Kaestner, A.P. Monaghan, G. Schutz, The mouse homolog of the region specific homeotic gene spalt of *Drosophila* is expressed in the developing nervous system and in mesoderm-derived structures, Mech. Dev. 56 (1996) 117–128.
[12] T. Ott, M. Parrish, K. Bond, A. Schwaeger-Nickolenko, A.P. Monaghan, A new member of the spalt like zinc finger protein family, Msal-3, is expressed in the CNS and sites of epithelial/mesenchymal interaction, Mech. Dev. 101 (2001) 203–207.
[13] J. Kohlhase, M. Heinrich, L. Schubert, M. Liebers, A. Kispert, F. Laccone, P. Turnpenny, R.M. Winter, W. Reardon, Okihiro syndrome is caused by SALL4 mutations, Hum. Mol. Genet. 11 (2002) 2979–2987.
[14] R. Al-Baradie, K. Yamada, C. St Hilaire, W.M. Chan, C. Andrews, N. McIntosh, M. Nakano, E.J. Martonyi, W.R. Raymond, S. Okumura, M.M. Okihiro, E.C. Engle, Duane radial ray syndrome (Okihiro syndrome) maps to 20q13 and results from mutations in SALL4, a new member of the SAL family, Am. J. Hum. Genet. 71 (2002) 1195–1199.
[15] J. Kohlhase, M. Heinrich, M. Liebers, L. Frohlich Archangelo, W. Reardon, A. Kispert, Cloning and expression analysis of

SALL4, the murine homologue of the gene mutated in Okihiro syndrome, Cytogenet. Genome Res. 98 (2002) 274–277.
[16] J. Kohlhase, A. Wischermann, H. Reichenbach, U. Froster, W. Engel, Mutations in the SALL1 putative transcription factor gene cause Townes–Brocks syndrome, Nat. Genet. 18 (1998) 81–83.
[17] R. Nishinakamura, Y. Matsumoto, K. Nakao, K. Nakamura, A. Sato, N.G. Copeland, D.J. Gilbert, N.A. Jenkins, S. Scully, D.L. Lacey, M. Katsuki, M. Asashima, T. Yokota, Murine homolog of SALL1 is essential for ureteric bud invasion in kidney development, Development 128 (2001) 3105–3115.
[18] R.P. Kuhnlein, G. Frommer, M. Friedrich, M. Gonzalez-Gaitan, A. Weber, J.F. Wagner-Bernholz, W.J. Gehring, H. Jackle, R. Schuh, Spalt encodes an evolutionarily conserved zinc finger protein of novel structure which provides homeotic gene function in the head and tail region of the *Drosophila* embryo, EMBO J. 13 (1994) 168–179.
[19] S.M. Kiefer, B.W. McDill, J. Yang, M. Rauchman, Murine Sall1 represses transcription by recruiting a histone deacetylase complex, J. Biol. Chem. 277 (2002) 14869–14876.
[20] C. Netzer, L. Rieger, A. Brero, C.D. Zhang, M. Hinzke, J. Kohlhase, S.K. Bohlander, SALL1, the gene mutated in Townes–Brocks syndrome, encodes a transcriptional repressor which interacts with TRF1/PIN2 and localizes to pericentromeric heterochromatin, Hum. Mol. Genet. 10 (2001) 3017–3024.
[21] D. Nellen, R. Burke, G. Struhl, K. Basler, Direct and long-range action of a DPP morphogen gradient, Cell 85 (1996) 357–368.
[22] M. Llimargas, Wingless and its signalling pathway have common and separable functions during tracheal development, Development 127 (2000) 4407–4417.
[23] T. Chihara, S. Hayashi, Control of tracheal tubulogenesis by Wingless signaling, Development 127 (2000) 4433–4442.
[24] H. Niwa, K. Yamamura, J. Miyazaki, Efficient selection for high-expression transfectants with a novel eukaryotic vector, Gene 108 (1991) 193–199.
[25] T. Matsuda, T. Nakamura, K. Nakao, T. Arai, M. Katsuki, T. Heike, T. Yokota, STAT3 activation is sufficient to maintain an undifferentiated state of mouse embryonic stem cells, EMBO J. 18 (1999) 4261–4269.
[26] I. Sakamoto, S. Kishida, A. Fukui, M. Kishida, H. Yamamoto, S. Hino, T. Michiue, S. Takada, M. Asashima, A. Kikuchi, A novel beta-catenin-binding protein inhibits beta-catenin-dependent Tcf activation and axis formation, J. Biol. Chem. 275 (2000) 32871–32878.
[27] Y. Watanabe, T. Tanaka, Y. Uchiyama, T. Takeno, A. Izumi, H. Yamashita, J. Kumakura, H. Iwanari, J. Shu-Ying, M. Naito, D.J. Mangelsdorf, T. Hamakubo, T. Kodama, Establishment of a monoclonal antibody for human LXRalpha: detection of LXRalpha protein expression in human macrophages, Nucl. Recept. 1 (2003) 1.
[28] S. Shibamoto, K. Higano, R. Takada, F. Ito, M. Takeichi, S. Takada, Cytoskeletal reorganization by soluble Wnt-3a protein signalling, Genes Cells 3 (1998) 659–670.
[29] T. Imamura, M. Takase, A. Nishihara, E. Oeda, J. Hanai, M. Kawabata, K. Miyazono, Smad6 inhibits signalling by the TGF-beta superfamily, Nature 389 (1997) 622–626.
[30] W. Ishida, T. Hamamoto, K. Kusanagi, K. Yagi, M. Kawabata, K. Takehara, T.K. Sampath, M. Kato, K. Miyazono, Smad6 is a Smad1/5-induced smad inhibitor. Characterization of bone morphogenetic protein-responsive element in the mouse Smad6 promoter, J. Biol. Chem. 275 (2000) 6075–6079.
[31] K. Nakajima, Y. Yamanaka, K. Nakae, H. Kojima, M. Ichiba, N. Kiuchi, T. Kitaoka, T. Fukada, M. Hibi, T. Hirano, A central role for Stat3 in IL-6-induced regulation of growth and differentiation in M1 leukemia cells, EMBO J. 15 (1996) 3651–3658.
[32] H. de The, M.M. Vivanco-Ruiz, P. Tiollais, H. Stunnenberg, A. Dejean, Identification of a retinoic acid responsive element in the retinoic acid receptor beta gene, Nature 343 (1990) 177–180.
[33] C. Sharpe, N. Lawrence, A. Martinez Arias, Wnt signalling: a theme with nuclear variations, Bioessays 23 (2001) 311–318.
[34] S.M. Kiefer, K.K. Ohlemiller, J. Yang, B.W. McDill, J. Kohlhase, M. Rauchman, Expression of a truncated Sall1 transcriptional repressor is responsible for Townes–Brocks syndrome birth defects, Hum. Mol. Genet. 12 (2003) 2221–2227.
[35] S. Marlin, S. Blanchard, R. Slim, D. Lacombe, F. Denoyelle, J.L. Alessandri, E. Calzolari, V. Drouin-Garraud, F.G. Ferraz, A. Fourmaintraux, N. Philip, J.E. Toublanc, C. Petit, Townes–Brocks syndrome: detection of a SALL1 mutation hot spot and evidence for a position effect in one patient, Hum. Mutat. 14 (1999) 377–386.
[36] D. Sweetman, T. Smith, E.R. Farrell, A. Chantry, A. Munsterberg, The conserved glutamine-rich region of chick csal1 and csal3 mediates protein interactions with other spalt family members. Implications for Townes–Brocks syndrome, J. Biol. Chem. 278 (2003) 6560–6566.
[37] A. Wodarz, R. Nusse, Mechanisms of Wnt signaling in development, Annu. Rev. Cell Dev. Biol. 14 (1998) 59–88.
[38] J. Koipally, E.J. Heller, J.R. Seavitt, K. Georgopoulos, Unconventional potentiation of gene expression by Ikaros, J. Biol. Chem. 277 (2002) 13007–13015.
[39] J. Koipally, J. Kim, B. Jones, A. Jackson, N. Avitahl, S. Winandy, M. Trevisan, A. Nichogiannopoulou, C. Kelley, K. Georgopoulos, Ikaros chromatin remodeling complexes in the control of differentiation of the hemo-lymphoid system, Cold Spring Harb. Symp. Quant. Biol. 64 (1999) 79–86.
[40] K.E. Brown, S.S. Guest, S.T. Smale, K. Hahm, M. Merkenschlager, A.G. Fisher, Association of transcriptionally silent genes with Ikaros complexes at centromeric heterochromatin, Cell 91 (1997) 845–854.
[41] J. Kim, S. Sif, B. Jones, A. Jackson, J. Koipally, E. Heller, S. Winandy, A. Viel, A. Sawyer, T. Ikeda, R. Kingston, K. Georgopoulos, Ikaros DNA-binding proteins direct formation of chromatin remodeling complexes in lymphocytes, Immunity 10 (1999) 345–355.
[42] B.S. Cobb, S. Morales-Alcelay, G. Kleiger, K.E. Brown, A.G. Fisher, S.T. Smale, Targeting of Ikaros to pericentromeric heterochromatin by direct DNA binding, Genes Dev. 14 (2000) 2146–2160.
[43] A. Bauer, S. Chauvet, O. Huber, F. Usseglio, U. Rothbacher, D. Aragnol, R. Kemler, J. Pradel, Pontin52 and reptin52 function as antagonistic regulators of beta-catenin signalling activity, EMBO J. 19 (2000) 6121–6130.
[44] T. Kramps, O. Peter, E. Brunner, D. Nellen, B. Froesch, S. Chatterjee, M. Murone, S. Zullig, K. Basler, Wnt/wingless signaling requires BCL9/legless-mediated recruitment of pygopus to the nuclear beta-catenin–TCF complex, Cell 109 (2002) 47–60.
[45] K. Tago, T. Nakamura, M. Nishita, J. Hyodo, S. Nagai, Y. Murata, S. Adachi, S. Ohwada, Y. Morishita, H. Shibuya, T. Akiyama, Inhibition of Wnt signaling by ICAT, a novel beta-catenin-interacting protein, Genes Dev. 14 (2000) 1741–1749.
[46] K. Takemaru, S. Yamaguchi, Y.S. Lee, Y. Zhang, R.W. Carthew, R.T. Moon, Chibby, a nuclear beta-catenin-associated antagonist of the Wnt/Wingless pathway, Nature 422 (2003) 905–909.
[47] R.A. Cavallo, R.T. Cox, M.M. Moline, J. Roose, G.A. Polevoy, H. Clevers, M. Peifer, A. Bejsovec, *Drosophila* Tcf and Groucho interact to repress Wingless signalling activity, Nature 395 (1998) 604–608.
[48] J. Roose, H. Clevers, TCF transcription factors: molecular switches in carcinogenesis, Biochim. Biophys. Acta 1424 (1999) M23–M37.
[49] N. Barker, A. Hurlstone, H. Musisi, A. Miles, M. Bienz, H. Clevers, The chromatin remodelling factor Brg-1 interacts with beta-catenin to promote target gene activation, EMBO J. 20 (2001) 4935–4943.

[50] R.T. Collins, J.E. Treisman, Osa-containing Brahma chromatin remodeling complexes are required for the repression of wingless target genes, Genes Dev. 14 (2000) 3140–3152.
[51] S. Sachdev, L. Bruhn, H. Sieber, A. Pichler, F. Melchior, R. Grosschedl, PIASy, a nuclear matrix-associated SUMO E3 ligase, represses LEF1 activity by sequestration into nuclear bodies, Genes Dev. 15 (2001) 3088–3103.
[52] H. Yamamoto, M. Ihara, Y. Matsuura, A. Kikuchi, Sumoylation is involved in beta-catenin-dependent activation of Tcf-4, EMBO J. 22 (2003) 2047–2059.
[53] C. Netzer, S.K. Bohlander, L. Rieger, S. Muller, J. Kohlhase, Interaction of the developmental regulator SALL1 with UBE2I and SUMO-1, Biochem. Biophys. Res. Commun. 296 (2002) 870–876.

F. Sato
I. Narita
S. Goto
D. Kondo
N. Saito
J. Ajiro
D. Saga
A. Ogawa
M. Kadomura
F. Akiyama
Y. Kaneko
M. Ueno
M. Sakatsume
F. Gejyo

Transforming growth factor-β1 gene polymorphism modifies the histological and clinical manifestations in Japanese patients with IgA nephropathy

Key words:
gene polymorphism; glomerulonephritis; IgA nephropathy; TGF-β1

Acknowledgments:
This work was supported in part by a Health and Labour Science Research Grants for Research on Specific Diseases from the Ministry of Health, Labour, and Welfare of Japan to Gejyo F. The authors thank Kumiko Furui and Naofumi Imai for excellent technical assistance.

Abstract: Transforming growth factor (TGF)-β1, a multifunctional cytokine, which regulates proliferation and differentiation of a variety of cell types, has the central role in the development and progression of renal injury in both animal models and human. Although it has been suggested that genetic variations in the *TGF-β1* gene are associated with the activity of the gene product, their clinical significance in glomerular disease is unknown. We investigated whether the polymorphisms of *C-509T* and *T869C* in *TGF-β1* account for interindividual variation in manifestations of IgA nephropathy (IgAN) using 626 Japanese subjects including 329 patients with histologically proven IgAN and 297 healthy controls with normal urinalysis. The frequencies of genotypes, alleles, and major haplotypes were similar between the patients and controls. The *C-509T* and *T869C* polymorphisms were in tight linkage disequilibrium, and the major haplotypes were *C-C* and *T-T*, which accounted for more than 95% of the total. In patients with *-509CC* and in those with the *869CC*, urinary protein excretion was higher than in those with other genotypes, whereas no difference in other clinical manifestations was noted. Moreover, patients with *-509CC* and those with *869CC* genotypes presented with a significant higher score of mesangial cell proliferation than in those with other genotypes. These results suggest that TGF-β1 gene polymorphisms are specifically associated with heavy proteinuria and mesangial cell proliferation in Japanese patients with IgAN, although they do not confer susceptibility to this disease.

Authors' affiliation:

F. Sato,
I. Narita,
S. Goto,
D. Kondo,
N. Saito,
J. Ajiro,
D. Saga,
A. Ogawa,
M. Kadomura,
F. Akiyama,
Y. Kaneko,
M. Ueno,
M. Sakatsume,
F. Gejyo

Division of Clinical Nephrology and Rheumatology, Niigata University Graduate School of Medical and Dental Sciences, Niigata, Japan

Correspondence to:
Ichiei Narita
Division of Clinical Nephrology and Rheumatology
Niigata University
Graduate School of Medical and Dental Sciences
1-754, Asahimachi-dori
Niigata 951-8510
Japan
Tel.: +81-25-227-2193
Fax: +81-25-227-0775
e-mail: narital@med.niigata-u.ac.jp

Transforming growth factor-β1 (TGF-β1) is a multifunctional cytokine, which regulates proliferation and differentiation of a wide variety of cell types. *In vitro* studies have suggested that mesangial matrix accumulation, increased fibrosis, and cell proliferation are promoted by TGF-β1 (1, 2) The central role of this cytokine in the development and progression of renal injury has been well documented in both animal models and human diseases (3). Recent evidence indicates the functional roles of TGF-β1 signaling in mediating apoptosis and epithelial-to-mesenchymal transdifferentiation, which have been proposed as putative primary pathomechanisms of progression of renal disease (4). In addition to the central roles of this

Received 9 December 2003, revised 24 February 2004, accepted for publication 24 March 2004

doi: 10.1111/j.1399-0039.2004.00256.x

Tissue Antigens 2004: 64: 35–42

cytokine in the progression of renal disease, TGF-β1 is known to be involved in the class switching to immunoglobulin (Ig)A in B-lymphocytes (5). Because it has been shown that the concentration of TGF-β1 is predominantly under genetic control (6, 7), genetic polymorphisms, which influence the gene transcription or the activity of TGF-β1, may account for the development, as well as the interindividual variation in manifestations of glomerular disease such as primary IgA nephropathy (IgAN).

IgAN, characterized by mesangial proliferative glomerulonephritis with predominant deposits of IgA in the glomerular mesangial area, is the most common form of primary glomerulonephritis, and one of the principal causes of end-stage renal disease (ESRD). Almost 40% of IgAN cases progress to ESRD during the initial 20 years after the onset, whereas the remaining patients have benign renal prognosis (8–10). It has been suggested that, both environmental and genetic factors are involved in the development and progression of this disease (11, 12).

The human gene encoding TGF-β1 (MIM 190180), located on chromosome 19q13, is highly polymorphic. Five polymorphisms in Caucasian populations have been identified: two in the promoter region at position −800 and −509, one at position +72 in a non-translated region, and two in the signal sequence at positions +869 and +915, which change codon 10 (T or C, leucine→proline) and codon 25 (G or C, arginine→proline), respectively (6). For codon 25, the C alelle encoding proline for these polymorphisms is associated with lower TGF-β1 synthesis *in vitro* and *in vivo*. However, there is no gene variation at codon 25 in Japanese (13, 14). In this study, we evaluated two polymorphisms, *C-509T* and *C869T* of *TGF-β1*, because both of them have been reported to be associated with some clinical phenotypes (15–19). Grainger et al. (7) found that the *C-509T* polymorphism was associated with the circulating concentration of TGF-β1, which was significantly lower in subjects with *CC* genotype than with other genotypes in Caucasian women. On the other hand, *CC* genotype of the *T869C* polymorphism was associated with higher TGF-β1 concentration than other genotypes in Japanese (18, 19).

Little is known about the linkage disequilibrium between these two genetic polymorphisms, or their significance in the patients with IgAN. Therefore, in this study, we have investigated the possible association of genetic polymorphism of *C-509T* and *T869C* in *TGF-β1* with the development, as well as the clinical and histopathological manifestations, in Japanese patients with IgAN.

Materials and methods

Study subjects

The ethics committee of our institution approved the protocol for the study, and informed written consent for the genetic studies was obtained from all participants. Japanese patients were eligible for inclusion in the analysis when (1) they had been diagnosed as having IgAN by kidney biopsy at our institute between 1976 and 2002 (2), they had no evidence of systemic diseases such as hepatic glomerulosclerosis, Schönlein-Henoch purpura, and rheumatoid arthritis (3), written informed consent for genetic study was obtained. Among 4587 patients who underwent renal biopsy at our institute between 1976 and 2002, 582 were diagnosed as having IgAN. In total, 329 patients fulfilled the above criteria and were recruited for this study. In all cases, the diagnosis of IgAN was based on a kidney biopsy that revealed the presence of dominant or codominant glomerular mesangial deposits of IgA as assessed by immunofluorescence. The majority of the 253 patients, who did not enter the study, were not included because written informed consent for genetic study was not available.

To provide a control for the local genotype frequency being examined, 297 Japanese volunteers (146 female and 151 male) aged 40 years or older with no history of renal disease and with normal urinalysis were also recruited.

Clinical and histological manifestations

Clinical characteristics of the patients with IgAN at the time of diagnosis including gender, age, body mass index (BMI), urinary protein excretion (g/24 h), serum creatinine (sCr, mg/dl), 24-h creatinine clearance (Ccr, ml/min), serum IgA (mg/dl), and office blood pressures were investigated from their medical records. The time from the first urine abnormality to renal biopsy (month) was also recorded for 245 of the 329 patients, where the first episode of urine abnormality (proteinuria or hematuria) could be clearly defined.

Histopathological findings were classified according to the classification described previously (20). A single pathologist evaluated all specimens by light microscopy in a double blind fashion. Glomerular changes were scored for each glomerulus, and the average score of each patient was calculated. The scores for cellular proliferation and the matrix increase in the mesangium were graded from zero to four as follows: grade 0, no light-microscopic abnormalities; grade 1, segmental mild proliferation of mesangial components; grade 2, segmental moderate or global mild proliferation of mesangial components; grade 3, segmental sclerosis or global moderate proliferation of mesangial components; and grade 4, global sclerosis or global marked proliferation of mesangial components.

Other glomerular changes including endocapillary proliferation, duplication of glomerular basement membrane (GBM), crescent formation, and adhesion of tufts to Bowman's capsule as well as tubulointerstitial lesions were graded from zero to four according to their

incidence as follows: 0–4%, 5–24%, 25–49%, 50–74%, and 75–100%.

Measurement of serum TGF-β1 concentration

We could examine serum sample at the time of biopsy, before any specific treatment performed, from only a portion of the patients studied. In 78 patients with IgAN, whose serum samples at the time of diagnosis were available, serum levels of TGF-β1 were measured by an enzyme-linked immunosorbent assay (ELISA) kit (Amersham Bioscience, Pisctaway, NJ). According to the manufacturer's instruction manual, the detection limit of this assay was 4 pg/ml, and the intra-assay and interassay coefficients of variance were ≤3.9 and ≤13.4%, respectively. The assay showed essentially no cross-reactivity (≤1%) with TGF β2, TGF β3, or other cytokines.

Genotype determination

Genomic DNA of peripheral blood cells was isolated by an automatic DNA isolation system (NA-1000; Kurabo, Osaka, Japan). The genotypes of *C-509T* and *T869C* of *TGF β1* gene were determined by polymerase chain reaction-restriction fragment polymorphism (PCR-RFLP) as described previously (17, 21). PCR primers for the *C-509T* polymorphism were 5′-GGGGACACCATCTACAGTG-3′ (forward) and 5′-GGAGGAGGGGGCAA CAGG-3′ (reverse), and those for *T869C* were 5′-TTCAAGACCACCCACCT TCT-3′ (forward) and 5′-TCGCGGGTGCTGTTGT ACA-3′ (reverse), respectively. The reaction mixture contained 1 × PCR buffer, 1.5 mmol/l $MgCl_2$, 200 mmol/l deoxynucleotide triphosphates (dNTPs), 1unit Taq DNA polymerase (Takara, Kyoto, Japan), 10 pmol of each primer, and 50–100 ng of genomic DNA. The PCR amplification reaction consisted of a cycle at 94°C for 5 min, followed by 35 cycles of denaturation at 94°C for 30 s, annealing at 64°C for 30 s (*C-509T*) or at 60°C for 30 s (*T869C*), and extension at 72°C for 1 min. A final extension was performed at 72°C for 5 min. The PCR products were digested with restriction endonuclease *Eco*81I (MBI Fermentas, Hanover, MD) for *C-509T* and *Msp*AlI (New England Biolabs Inc., Beverly, MA) for *T869C*, respectively, and electrophoresed on a polyacrylamide gel. The gel was silver stained with using the DNA Silver Staining Kit (Pharmacia Biotech, Pisctaway, NJ). For *C-509T* polymorphism, the T alleles resulted in a 430-bp and 25-bp fragment, whereas the 455-bp – *509C* alleles lacked its restrictive site (Fig. 1A). For *T*869C polymorphism, 273-bp and 12-bp fragment were detected for 869C alleles, whereas 285-bp *869T* alleles lacked its restrictive site, and the complete digestion was confirmed by disappearance of the 500-bp band, which corresponded to the PCR product without *MSP*AlI digestion (Fig. 1B).

Haplotype estimation and statistical analysis

Haplotype frequencies for sets of alleles were estimated using ARLEQUIN software Ver 2.0, which was based on the maximum likelihood method (Genetics and Biometry Laboratory, Department of Anthropology, University of Geneva, Geneva, Switzerland; http://www.lgb.unige.ch/arlequin/). Pairwise linkage disequilibrium coefficients (D′) were also

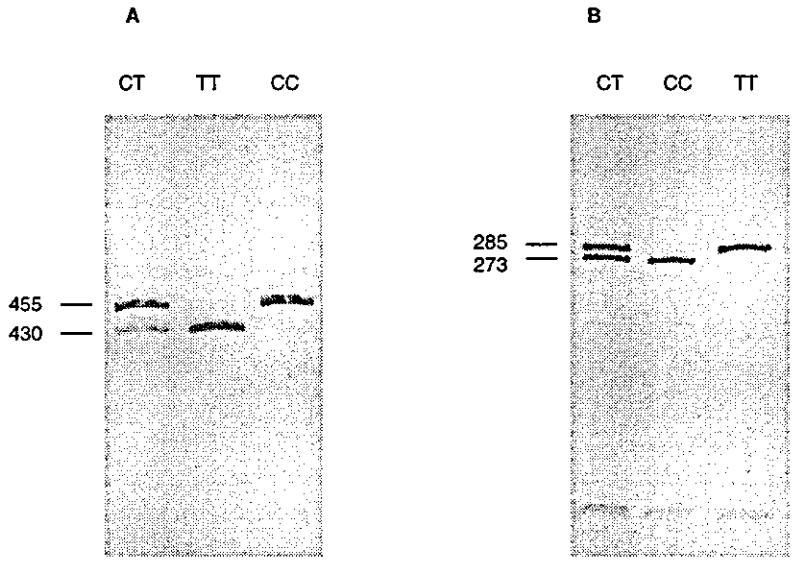

Fig. 1. **Polyacrylamide gel elecrophoresis of PCR products after restriction digestion.** Each genotype of *C-509T* (A) and *T869C* (B) was clearly defined by the method described.

calculated using ARLEQUIN Ver 2.0 and expressed as the D′ = D/Dmax, according to Slatkin (22).

STATVIEW 5.0 statistical software (Abacus Concepts, Inc., Berkeley, CA) was used for statistical analyzes. Hardy–Weinberg equilibrium was tested by a χ^2-test with 1 d.f. Clinical data were compared between different genotypes of both *–509* and *869* positions by Kruskal–Wallis test or Mann–Whitney *U*-test. Values of $P < 0.05$ were considered to indicate statistical significance. When it was significant by Kruskal–Wallis test, we performed the Mann–Whitney *U*-test to compare each pair of genotype groups, adjusting by Bonferoni correction, where $P < 0.0167$ was considered statistically significant.

Results

In total, we genotyped 626 subjects, which consisted of 329 patients with histologically proven IgAN and 297 healthy controls. Table 1 summarizes the genotype distributions, allele frequencies, and estimated haplotype frequencies of *C-509T* and *T869C* polymorphisms of *TGF-β1* gene in patients with IgAN and normal controls. The genotype distributions were similar between the patients with IgAN and controls, and the allele frequencies were in accordance with previous reports in a Japanese population (19). The expected frequencies of the genotypes, assumed to be under Hardy–Weinberg equilibrium, were no different from the observed genotype distributions in both the patients with IgAN and the controls (data not shown). We found that the *C-509T* and *T869C* polymorphisms were in tight linkage disequilibrium (D′ = 0.9401; $P < 0.0001$) and that the major haplotypes for these two loci were *C-C* and *T-T*, which accounted for more than 95% of the total chromosomes. The frequencies of these two major haplotypes were similar between patients with IgAN and healthy controls.

Genotype distributions, allele frequencies, and estimated haplotype frequencies of *C-509T* and *T869C* polymorphisms of *TGF-β1* gene in patients with IgAN and normal controls

			IgAN (n = 329)	Control (n = 297)	P-value	χ^2
C-509T	Genotype	*CC*	89 (0.271)	76 (0.256)		
		CT	174 (0.529)	157 (0.529)		
		TT	66 (0.201)	64 (0.215)	0.8637	0.293
	Allele	*C*	0.535	0.520		
		T	0.465	0.480	0.6809	0.169
T869C	Genotype	*CC*	86 (0.261)	80 (0.269)		
		CT	167 (0.508)	152 (0.512)		
		TT	76 (0.231)	65 (0.219)	0.9301	0.145
	Allele	*C*	0.515	0.525		
		T	0.485	0.475	0.7722	0.084
Estimated haplotype of *C-509T* and *T869C*						
	-509	869				
	C	*C*	0.501	0.515	0.6300	0.232
	T	*T*	0.451	0.470	0.5158	0.422
	Others		0.048	0.015		

IgAN, IgA nephropathy.

Table 1

Table 2 summarizes the demographic data and clinical characteristics at the time of diagnosis among IgAN patients with each genotype of the *C-509T* and *T869C* polymorphisms. There was no significant difference among patients with each genotype of both polymorphisms in gender, age, height, weight, and time from the first urine abnormality to renal biopsy, serum creatinine, creatinine clearance, serum IgA, or blood pressures. However, in patients with *CC* genotype of *C-509T* polymorphism and in those with the *CC* of *T869C*, urinary protein excretion was significantly higher than in those with other genotypes (Kruskal–Wallis test, $P = 0.0051$ for *C-509T*, and $P = 0.0241$ for *T869C*). Even after Bonferoni correction in the Mann–Whitney *U*-test, patients with the *–509CC* and *869CC* genotypes had significantly higher urinary protein excretion than those with *–509CT* ($P = 0.0011$) and *869CT* ($P = 0.0038$), respectively. Although the differences were no longer significant after Bonferoni correction between *–509CC vs –509TT* ($P = 0.0178$) and *869CC vs 869TT* ($P = 0.0853$), we further examined the association between these polymorphisms in the incidence of proteinuria of 1.0 g/day or more. The percentage of patients with urinary protein excretion of 1.0 g/day or more was significantly higher in patients with the *–509CC* ($\chi^2 = 11.003$, $P = 0.0041$) and those with the *869CC* of *TGF-β1* polymorphism ($\chi^2 = 9.382$, $P = 0.0092$) than in those with other genotypes. Table 3 summarizes estimated haplotype frequencies in patients with or without urinary protein excretion of 1.0 g/day or more. The *C-C* haplotype of these polymorphisms was significantly more frequent in patients with urinary protein excretion of 1.0 g/day or more than in those with less proteinuria ($\chi^2 = 11.782$, $P = 0.0006$).

Next, we investigated possible association between the *TGF-β1* polymorphisms and histopathological findings of kidney biopsy including glomerular and interstitial changes. Figures 1 and 2 show the mean scores for mesangial cell proliferation, mesangial matrix increase, endocapillary proliferation, duplication of GBM, crescent formation, adhesion of tufts to Bowman's capsule, and tubulointerstitial lesions in patients with each genotype of *TGF-β1*. Glomerular cell proliferation was significantly higher in patients with the *–509CC* (Fig. 1, Mann–Whitney *U*-test, $P = 0.0054$) and with the *869CC* genotype (Fig 2, $P = 0.0052$) than that in those with other genotypes, whereas no difference was detected in terms of any other histopathological scores (data not shown). Moreover, the

Demographic data and clinical characteristics at time of diagnosis among patients with each genotype of the C-509T and T869C polymorphisms

		C-509T				*T869C*			
	Total ($n=329$)	CC ($n=89$)	CT ($n=174$)	TT ($n=66$)	*P*-value	CC ($n=86$)	CT ($n=167$)	TT ($n=76$)	*P*-value
Gender (male/female)	149/180	48/41	75/99	26/40	0.1675	41/45	77/90	31/45	0.8950
Age (years)	36.9±13.8	36.8±13.3	37.1±13.8	37.3±14.8	0.9958	36.8±12.9	37.5±14.1	36.5±14.3	0.8682
Height (cm)	161.1±9.5	160.5±10.9	161.4±8.9	161.4±8.4	0.9845	160.7±9.6	161.9±8.7	160.0±10.5	0.4418
Weight (kg)	58.8±9.7	59.7±10.2	58.5±9.7	58.3±9.7	0.3924	59.8±9.3	58.7±9.8	57.9±10.5	0.5103
Urinary protein (UP) excretion (g/day)	1.39±1.52	1.74±1.67	1.27±1.54	1.27±0.17	0.0051	1.67±1.67	1.25±1.54	1.39±1.42	0.0241
Patients with UP of 1.0 g/day or more (%)	48.3	62.8	41.3	47.5	0.0041	60.5	41.6	49.3	0.0092
Serum creatinine (mg/dl)	0.98±0.59	0.97±0.44	1.02±0.63	0.94±0.70	0.2125	0.95±0.44	1.02±0.63	0.96±0.69	0.3180
Creatinine clearance (ml/min)	88.8±32.6	91.1±31.6	85.0±31.7	95.5±35.0	0.1293	91.9±32.0	85.4±31.0	92.6±35.6	0.2677
Systolic blood pressure (mmHg)	128.3±18.8	129.5±21.2	127.9±18.2	126.7±16.4	0.8989	129.3±21.5	127.7±18.3	127.4±16.2	0.9948
Diastolic blood pressure (mmHg)	77.4±13.7	77.3±13.0	77.9±13.8	75.9±13.6	0.6679	76.9±13.6	77.6±13.7	77.0±13.4	0.8799
Serum IgA concentration (mg/dl)	355.6±115.8	375.5±138.7	349.7±105.7	360.6±122.1	0.5447	374.6±135.5	350±108.7	359.2±121.0	0.4978
Time from the first urine abnormality to renal biopsy (years)	5.2±6.3	5.6±7.2	4.9±6.1	5.2±6.1	0.6029	5.7±7.2	5.0±6.1	4.8±6.0	0.5228

Table 2

prevalence of cases with cell proliferation of grade 2 (diffuse mild) or more was significantly higher in patients with the *-509CC* ($\chi^2=7.095$, $P=0.0077$) and with *869CC* genotype of *TGF-β1* ($\chi^2=5.651$, $P=0.0172$) than in those with other genotypes.

Because several investigators have already reported associations between TGF-β1 gene polymorphisms and the circulating level of TGF-β1 in non-nephritic populations (6, 7, 18, 19), the circulating level of TGF-β1 in patients with IgAN was investigated in this study

Estimated haplotype frequencies in patients with or without urinary protein excretion of 1.0 g/day or more

	Urinary protein of 1.0 g/day or more			
Estimated haplotype of −509 and 869 loci	Yes ($n=318$)	No ($n=390$)	χ^2	*P*-value
C-C	181	148	11.78	0.0006
T-T	123	175	10.85	0.0010
Others	14	17	-	-

Table 3

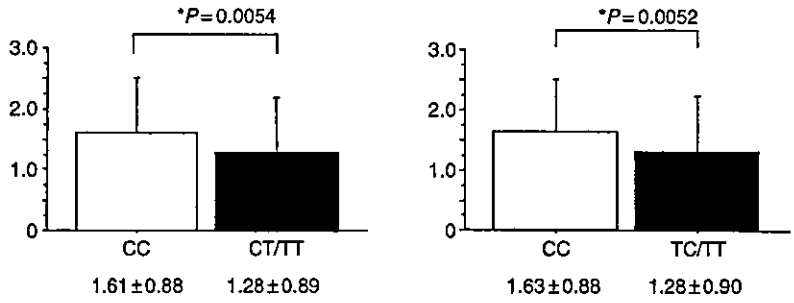

Fig. 2. **Mean values of mesangial cell proliferation in IgA nephropathy (IgAN) patients with the *CC* (□) and *TC/TT* (■) genotypes of the *TGF-β1 C-509T* (A) *and T869C* (B) polymorphisms.** Glomerular changes were scored for each glomerulus, and the mean score of each was calculated. The scores for mesangial cell proliferation were graded from zero to four as described in Method. Data are given as mean ± SD. *$P<0.05$ by Mann–Whitney *U*-test.

by ELISA. In only 78 patients, the serums at the time of biopsy were available before any specific treatment. There was no significant difference in serum TGF-β1 concentrations among each genotype of *C-509T* and *T869C* (data not shown).

Discussion

TGF-β1 is an attractive and promising candidate for genetic studies of glomerular diseases, because this cytokine has been well documented to be one of the key mediators contributing to the initiation and progression of renal injury and the production of TGF-β1 has been reported to be under genetic control (6, 7). Moreover, this cytokine acts on B-lymphocytes in IgA class switching. Therefore, this study examined possible associations between the genetic polymorphisms of *TGF-β1* and the development of IgAN, as well as the clinical and histopathological manifestations of patients with histologically proven IgAN. There was no difference in genotype, allele frequencies, or estimated major haplotype frequencies of these polymorphisms between IgAN patients and healthy controls, indicating that the *TGF-β1* polymorphisms investigated in the present study have no major involvement in the initiation of IgAN, while they were associated with heavy proteinuria and mesangial cell proliferation within patients with IgAN. This may support the notion that the impact of polymorphisms on phenotype depends on the specific disease under study.

Both polymorphisms investigated in this study, *C-509T* and *T869C* in the *TGF-β1* gene, have been reported to be associated with the transcriptional activity of the gene or the serum level of the gene product (7, 19). Although *G915C* polymorphism, which results in the change of codon 25 from arginine to proline, is another gene variation in the first exon of *TGF-β1* and is the best evaluated in Caucasian populations, it has been known that there is no C allele of this polymorphism in Japanese (13, 14).

The haplotype analysis revealed that *C-509T* and *T869C* loci are in tight linkage disequilibrium, and the major haplotypes were *C-C* and *T-T*. Although the present study could not confirm or completely refuse the possible association between these polymorphisms and circulating level of TGF-β1, our result is consistent with a report in a Japanese population (17). It would be more valuable to assess the local expression of TGF-β1 in the kidney, because TGF-β1 acts as an auto- or paracrine factor in local tissue injury rather than as a systemic circulating factor (3, 23). In fact, Melk et al. (24) have recently reported that the *T869C* polymorphism in *TGF-β1* was significantly associated with TGF-β1 mRNA expression in normal kidney but not in kidneys from chronic allograft nephropathy. Although it is important to prove the direct association between TGF-β1 gene variation and its expression in local renal tissue, in this study, we could not measure the TGF-β1 mRNA expression in the renal tissue, because this study was retrospective. In addition, it is assumed that immunohistological study is not sufficient for providing convincing and quantitative data, partly because of the large interglomerular variation.

The *T869C* and *C-509T* polymorphisms in *TGF-β1* were specifically associated with marked proteinuria in terms of clinical manifestations of IgAN. The incidence of proteinuria of 1.0 g/day or more was significantly higher in patients with *CC* genotype than in those with other genotypes of both *C-509T* and *T869C* polymorphisms. Moreover, *C-C* haplotype of these polymorphisms was significantly more frequent in patients with urinary protein excretion of 1.0 g/day or more than in those with less proteinuria. We have no data available indicating that the increased amount of urinary protein in *–509CC* and *869CC* genotype was due to increased activity of TGF-β1 in local tissue. However, there is evidence that, in glomerular podocytes, TGF-β1 increases the production of vascular endothelial growth factor (VEGF) (25), which has a role in enhancing vascular permeability via nitric oxide and prostacyclin (26), as well as in proteinuria (27, 28). In addition to the effect on VEGF expression, TGF-β1 has a substantial effect on collagen synthesis in glomerular podocytes. A relative increase in the α3-chain of collagen IV, which may alter the structure of the GBM and affect its function as a filtration barrier, has been reported in podocytes in response to TGF-β1 (25).

In the histopathological assessment, the associations of the *TGF-β1* genotypes were detected only with mesangial cell proliferation, whereas no significant association was observed with respect to any other histopathological features including mesangial matrix increase and interstitial fibrosis. We could not clarify the underling mechanism in which the association was restricted to mesangial cell proliferation. We hypothesized that the polymorphisms in *TGF-β1* would predominantly associate with mesangial matrix increase and interstitial fibrosis, because the expression of TGF-β1 has mainly been reported to be associated with extracellular matrix expansion and interstitial fibrosis (29). However, in addition, TGF-β1 is known to have dual effects on the proliferation of a variety of cells. Indeed, TGF-β1 at a low concentration promotes mesangial cell proliferation and at a high concentration suppresses it *in vitro* (30). Therefore, our findings suggest that both the *CC* genotype of *C-509T* and *T869C* polymorphisms of *TGF-β1* are associated with higher activity of TGF-β1 in glomeruli with inflammatory injury than in other genotypes, but the increased activity is the extent to which mesangial cell proliferation is stimulated. Alternatively, TGF-β1 also up-regulates production of platelet-derived growth factor (PDGF) (31), and in the kidney of TGF-β1 gene-transfected rats, mesangial cell proliferation increased with extracellular matrix expansion (32). Because PDGF

stimulates the proliferation of mesangial cells (33, 34), the present result may reflect the effect of TGF-β1 on PDGF expression in glomeruli. There is also a possibility that the influences of TGF-β1 on mesangial matrix increase and interstitial fibrosis were less detectable than mesangial cell proliferation in the method, which we employed for the assessment of histopathological changes. In fact, both scores for mesangial matrix increase and interstitial fibrosis were consistently, but not significantly, higher in the *CC* genotype of *C-509T* and *T869C* polymorphisms of *TGF-β1*. Although this study could not reveal the functional significance of the gene polymorphisms, the findings of this study suggest that both the *C-509T* and *T869C* polymorphisms have a direct or indirect influence on the transcriptional activity of the *TGF-β1* gene. There is also a possibility that these gene polymorphisms may be in linkage disequilibrium with an undefined gene variation, which affects the TGF-β1 activity in glomerular inflammatory injury.

In conclusion, the present results indicate that *CC-509* and *CC869* genotypes, as well as *C-C* haplotype, of TGF-β1 gene polymorphisms are specifically associated with marked proteinuria and increased mesangial cell proliferation, both of which are risk factors of progression to ESRD in Japanese patients with IgAN. Although a prospective randomized controlled study with a long-term observation is needed to establish the prognostic significance of these gene polymorphisms, this translational approach supports a concept that components in the secretion/activation of TGF-β1 may be a target of therapeutic strategies in the future.

References

1. Okuda S, Languino LR, Ruoslahti E, Border WA. Elevated expression of transforming growth factor-beta and proteoglycan production in experimental glomerulonephritis. Possible role in expansion of the mesangial extracellular matrix. *J Clin Invest* 1990: **86**: 453–62.
2. Border WA, Noble NA. Transforming growth factor beta in tissue fibrosis. *N Engl J Med* 1994: **331**: 1286–92.
3. Border WA, Ruoslahti E. Transforming growth factor-beta in disease: the dark side of tissue repair. *J Clin Invest* 1992: **90**: 1–7.
4. Bottinger EP, Bitzer M. TGF-beta signaling in renal disease. *J Am Soc Nephrol* 2002: **13**: 2600–10.
5. van Vlasselaer P, Punnonen J, de Vries JE. Transforming growth factor-beta directs IgA switching in human B cells. *J Immunol* 1992: **148**: 2062–7.
6. Awad MR, El-Gamel A, Hasleton P, Turner DM, Sinnott PJ, Hutchinson IV. Genotypic variation in the transforming growth factor-beta1 gene: association with transforming growth factor-beta1 production, fibrotic lung disease, and graft fibrosis after lung transplantation. *Transplantation* 1998: **66**: 1014–20.
7. Grainger DJ, Heathcote K, Chiano M et al. Genetic control of the circulating concentration of transforming growth factor type beta1. *Hum Mol Genet* 1999: **8**: 93–7.
8. Levy M, Berger J. Worldwide perspective of IgA nephropathy. *Am J Kidney Dis* 1988: **12**: 340–7.
9. Radford Jr MG, Donadio Jr JV, Bergstralh EJ, Grande JP. Predicting renal outcome in IgA nephropathy. *J Am Soc Nephrol* 1997: **8**: 199–207.
10. Maisonneuve P, Agodoa L, Gellert R et al. Distribution of primary renal diseases leading to end-stage renal failure in the United States, Europe, and Australia/New Zealand: results from an international comparative study. *Am J Kidney Dis* 2000: **35**: 157–65.
11. Hsu SI, Ramirez SB, Winn MP, Bonventre JV, Owen WF. Evidence for genetic factors in the development and progression of IgA nephropathy. *Kidney Int* 2000: **57**: 1818–35.
12. Galla JH. Molecular genetics in IgA nephropathy. *Nephron* 2001: **88**: 107–12.
13. Ohtsuka T, Yamakage A, Yamazaki S. The polymorphism of transforming growth factor-beta1 gene in Japanese patients with systemic sclerosis. *Br J Dermatol* 2002: **147**: 458–63.
14. Watanabe Y, Kinoshita A, Yamada T et al. A catalog of 106 single-nucleotide polymorphisms (SNPs) and 11 other types of variations in genes for transforming growth factor-beta1 (TGF-beta1) and its signaling pathway. *J Hum Genet* 2002: **47**: 478–83.
15. Baan CC, Balk AH, Holweg CT et al. Renal failure after clinical heart transplantation is associated with the TGF-beta 1 codon 10 gene polymorphism. *J Heart Lung Transplant* 2000: **19**: 866–72.
16. Lacha J, Hubacek JA, Potmesil P, Viklicky O, Malek I, Vitko S. TGF-beta I gene polymorphism in heart transplant recipients-effect on renal function. *Ann Transplant* 2001: **6**: 39–43.
17. Yamada Y, Miyauchi A, Takagi Y, Tanaka M, Mizuno M, Harada A. Association of the C-509→T polymorphism, alone of in combination with the T869→C polymorphism, of the transforming growth factor-beta1 gene with bone mineral density and genetic susceptibility to osteoporosis in Japanese women. *J Mol Med* 2001: **79**: 149–56.
18. Yamada Y, Miyauchi A, Goto J et al. Association of a polymorphism of the transforming growth factor-beta1 gene with genetic susceptibility to osteoporosis in postmenopausal Japanese women. *J Bone Miner Res* 1998: **13**: 1569–76.
19. Yokota M, Ichihara S, Lin TL, Nakashima N, Yamada Y. Association of a T29→C polymorphism of the transforming growth factor-beta1 gene with genetic susceptibility to myocardial infarction in Japanese. *Circulation* 2000: **101**: 2783–7.
20. Suzuki S, Sato H, Kobayashi H et al. Comparative study of IgA nephropathy with acute and insidious onset. Clinical, laboratory and pathological findings. *Am J Nephrol* 1992: **12**: 22–8.
21. Wood NA, Thomson SC, Smith RM, Bidwell JL. Identification of human TGF-beta1 signal (leader) sequence polymorphisms by PCR-RFLP. *J Immunol Methods* 2000: **234**: 117–22.
22. Slatkin M. Linkage disequilibrium in growing and stable populations. *Genetics* 1994: **137**: 331–6.
23. Taniguchi Y, Yorioka N, Masaki T, Asakimori Y, Yamashita K, Yamakido M. Localization of transforming growth factors beta1 and beta2 and epidermal growth factor in IgA nephropathy. *Scand J Urol Nephrol* 1999: **33**: 243–7.

24. Melk A, Henne T, Kollmar T et al. Cytokine single nucleotide polymorphisms and intrarenal gene expression in chronic allograft nephropathy in children. *Kidney Int* 2003: **64**: 314–20.
25. Iglesias-de la Cruz MC, Ziyadeh FN, Isono M et al. Effects of high glucose and TGF-beta1 on the expression of collagen IV and vascular endothelial growth factor in mouse podocytes. *Kidney Int* 2002: **62**: 901–13.
26. Murohara T, Horowitz JR, Silver M et al. Vascular endothelial growth factor/vascular permeability factor enhances vascular permeability via nitric oxide and prostacyclin. *Circulation* 1998: **97**: 99–107.
27. Cha DR, Kim NH, Yoon JW et al. Role of vascular endothelial growth factor in diabetic nephropathy. *Kidney Int Suppl* 2000: **77**: S104–12.
28. Hovind P, Tarnow L, Oestergaard PB, Parving HH. Elevated vascular endothelial growth factor in type 1 diabetic patients with diabetic nephropathy. *Kidney Int Suppl* 2000: **75**: S56–61.
29. Yoshioka K, Takemura T, Murakami K et al. Transforming growth factor-beta protein and mRNA in glomeruli in normal and diseased human kidneys. *Laboratory Invest* 1993: **68**: 154–63.
30. Mene P, Simonson MS, Dunn MJ. Physiology of the mesangial cell. *Physiol Rev* 1989: **69**: 1347–424.
31. Roberts AB, Sporn MB. Regulation of endothelial cell growth, architecture, and matrix synthesis by TGF-beta. *Am Rev Respir Dis* 1989: **140**: 1126–8.
32. Isaka Y, Fujiwara Y, Ueda N, Kaneda Y, Kamada T, Imai E. Glomerulosclerosis induced by in vivo transfection of transforming growth factor-beta or platelet-derived growth factor gene into the rat kidney. *J Clin Invest* 1993: **92**: 2597–601.
33. Betsholtz C, Raines EW. Platelet-derived growth factor: a key regulator of connective tissue cells in embryogenesis and pathogenesis. *Kidney Int* 1997: **51**: 1361–9.
34. Floege J, Eng E, Young BA et al. Infusion of platelet-derived growth factor or basic fibroblast growth factor induces selective glomerular mesangial cell proliferation and matrix accumulation in rats. *J Clin Invest* 1993: **92**: 2952–62.

Kidney International, Vol. 65 (2004), pp. 1135–1144

PERSPECTIVES IN RENAL MEDICINE

Relationship between tonsils and IgA nephropathy as well as indications of tonsillectomy

YUANSHENG XIE, XIANGMEI CHEN, SHINICHI NISHI, ICHIEI NARITA, and FUMITAKE GEJYO

Kidney Center of PLA, Department of Nephrology, Chinese General Hospital of PLA, Beijing, China; and Division of Clinical Nephrology and Rheumatology, Niigata University Graduate School of Medical and Dental Sciences, Niigata, Japan

Relationship between tonsils and IgA nephropathy as well as indications of tonsillectomy. Although there are many papers about IgA nephropathy (IgAN) and tonsils, respectively, reviews about the relationship between tonsils, tonsillitis, tonsillectomy, and IgAN are limited. In this review, we introduced the structure, development, and function of tonsils, difference of tonsils with and without IgAN, consistency of both tonsillar IgA and glomerular IgA, the effect of tonsil stimulation, tonsil infection, and tonsillectomy on IgAN showed some evidences in which tonsils were closely related to IgAN and polymeric IgA1 deposited in glomerular mesangium were at least in part of tonsillar origin. Tonsillectomy can improve the urinary findings, keep stable renal function, improve mesangial proliferation and IgA deposit, have a favorable effect on long-tern renal survival in some IgAN patients, and do not cause significant immune deficiency and do not increase incidence of the upper respiratory tract infections, and can be used as a potentially effective treatment. The indications of tonsillectomy in patients with IgAN include mainly the deterioration of urinary findings after tonsillar infection, mild or moderate renal damage. However, tonsillectomy may not be enough and may not change the prognosis in IgAN patients with marked renal damage.

Immunoglobulin A nephropathy (IgAN), that is, nephropathy with mesangial IgA-IgG deposits, was first reported by Berger and Hinglais in Frence in 1968 [1] and described by Berger in English in 1969 [2]. Studies for more than 30 years demonstrated that primary IgAN is an immune complex–mediated glomerulonephritis defined immunohistologically by the presence of glomerular IgA deposits [3]. It is now generally known to be the most common form of primary glomerulonephritis throughout the world [4–6]. Although primary IgAN was considered a benign condition for many years, it is now clear that a large number of cases eventually progress to renal failure [7–11]. Indeed, IgAN is the main cause of end-stage renal disease (ESRD) in patients with primary glomerular disease who require renal replacement therapy [12, 13]. However, the cause of primary IgAN, source of IgA deposited in glomeruli and the mechanism underlying mesangial IgA deposition in IgAN, is unclear and there is no effective treatment available for patients with IgAN [14].

The IgA deposited in glomerular mesangium in patients with IgAN appears to be exclusively of the IgA1 subclass [15] and IgA produced by tonsillar lymphcytes in patients with IgAN is mainly polymeric IgA1, about half of patients with IgAN their serum IgA levels increase [16] and tonsillectomy decreases the levels of serum IgA, suggesting there is any relationship between tonsils and IgAN. Recently, we demonstrated that the tonsillectomy has a favorable effect on long-term renal survival in patients with IgAN [17].

Although there are many papers about IgAN and tonsils, respectively, reviews about the relationship between tonsils, tonsillectomy, and IgAN are limited. In this review, we introduce the structure, development, and function of tonsils, difference of tonsils with and without IgAN, consistency of both tonsillar IgA and glomerular IgA, the effect of tonsil stimulation, tonsil infection, and tonsillectomy on IgAN, show some evidences in which tonsils were closely related to IgAN and polymeric IgA1 deposited in glomerular mesangium were at least in part of tonsillar origin, and present the indications of tonsillectomy in patients with IgAN.

STRUCTURE, DEVELOPMENT, AND FUNCTIONS OF TONSILS

Structure of tonsils

Human tonsils include the palatine tonsils, nasopharyngeal tonsil (adenoid), lingual tonsil and the tubal tonsils [18] (Fig. 1). The palatine tonsils are the largest ones in four types of tonsils in human beings. Histologically, tonsil tissues consist of four well-defined microcompartments,

Key words: tonsils, tonsillectomy, IgA nephropathy, treatment, indication.

Received for publication August 3, 2003
and in revised form September 28, 2003
Accepted for publication October 28, 2003

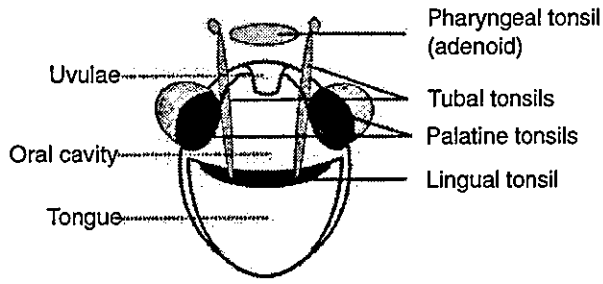

Fig. 1. Anatomy of the tonsils.

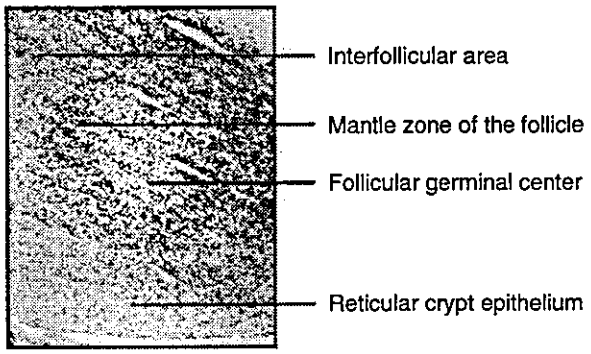

Fig. 2. Histologic structure of tonsils. The sample originated from tonsil tissues after tonsillectomy because of chronic tonsillitis in 8-year-old, male patient. The cellular nuclei of the section were stained with hematoxylin (original magnification ×50).

which all participate in the immune response: the reticular crypt epithelium, the interfollicular (extrafollicular) area, the mantle zone of lymphoid follicles, and the follicular germinal center [19] (Fig. 2). Cell biologically, immunocyts of tonsil tissues contain predominantly B cells (approximately 65%), approximately 30% $CD3^+$ T cells, and 5% macrophages. The T cells were primarily of the $CD4^+$ subset (approximately 80%) [20]. Quantitative immunohistochemistry reveals that IgG-containing B cells predominate in all lymphoid compartments, including follicles, extrafollicular areas, and reticular epithelium, whereas IgA cells are found predominantly in extrafollicular areas, especially subepithelial area, and IgM cells are in follicles. J chain is present within IgM and some IgA cells. The IgG:IgA:IgM class ratios of the overall tonsillar immunocyte population are 13:8:2. Cells containing IgD and IgE are rare [21]. In clinically normal tonsils, the overall percentage distribution of these cells is 65:30:3.5:1.2 for the IgG, IgA, IgM. and IgD classes, respectively. In recurrent tonsillitis, these figures are 53:39:4.7:4.4; in hyperplastic tonsillitis, 67:25:4.0:4.5; and in idiopathic tonsillar hyperplasia, 50:33:7.2:10, respectively [22]. In comparison with the clinically healthy tonsils, the number, the size of the germinal centers and the density of the immunocytes in tonsils are very large in the hyperplastic tonsils, large in chronic cryptic tonsillitis, but remarkably decreased in acute tonsillitis [23]. The study regarding the distribution and proportion of Ig subclasses producing cells in chronic tonsillitis show that the percentage ratios of IgG1:IgG2:IgG3:IgG4 were 53.1:35.9:4.7:6.3, respectively. Proportional ratios of IgA1:IgA2 are approximately 80:20 [24].

Development of tonsils

The development of the palatine tonsils starts during the 14th gestational week when the mesenchyme underlying the mucous membrane of the tonsillar cavity becomes invaded by mononuclear wandering cells. In fetuses of about the 16th gestational week epithelial crypts grow down into the connective tissue and are infiltrated by T lymphocytes. At the same time, precursors of interdigitating cells can be identified among the epithelial cells. Primary follicles develop in earlier fetal stages than in all other secondary lymphoid organs. They contain precursors of dendritic reticulum cells and lymphoid cells that belong to the B-cell line. These primary follicles may be considered as the first assemblage of B-cell regions in human fetal lymphoid tissue [25]. The formation of the follicular germinal centers reflecting B-cell activation by exogenous antigens takes place shortly after birth [26]. The immunohistochemical study show the morphometric features of tonsils below the age of 8 years are more active than those above the age of 8 years. Total number of IgA immunocytes is the highest at the age of 5 to 7 years with a decline by age. The serum IgA and salivary secretory IgA concentrations reach to adult's level at the age of 11 to 13 years. These results suggest that tonsils in preschool children are important as a local immunological defense mechanism [27].

Functions of tonsils

Tonsil tissues are located at the gateway of the respiratory and alimentary tract and belong to the mucosa-associated lymphoid tissue. The generation of B cells in the germinal centers of the tonsil is one of the most essential tonsillar functions. The major function of tonsils is as a first line of defense against viral, bacterial, and food antigens that enter the upper aerodigestive system. Secretory dimeric IgA produced by B cells has particular hydrophilic properties and is capable of preventing adsorption and penetration of bacteria and/or viruses into the upper respiratory tract mucosa [28]. With the uptake of antigen by microfold cells (membrane cell, M cells) present in the cryptepithelium a process is initiated, which ultimately results in the generation and dissemination of antigen-specific memory and mainly dimeric IgA-producing effector B lymphocytes. This process requires successful cognate interactions between antigen-presenting cells and lymphocytes and mutually between lymphocytes, which depend not only on antigen-specific